



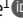




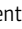





















ARTICLE

LACC1 deficiency links juvenile arthritis with autophagy and metabolism in macrophages

Ommar Omarjee^{1,2} , Anne-Laure Mathieu^{1,2} , Gaëlle Quiniou¹ , Marion Moreews¹ , Michelle Ainouze¹ , Cécile Frachette^{2,6} , Isabelle Melki^{2,3,4} , Cécile Dumaine³ , Mathieu Gerfaud-Valentin⁵ , Agnès Duquesne^{2,6} , Tilmann Kallinich⁷ , Eda Tahir Turanli^{8,9} , Christophe Malcus^{2,10} , Sébastien Viel^{2,11} , Rémi Pescarmona^{2,11} , Sophie Georjin-Lavialle^{17,18} , Yvan Jamilloux^{1,5} , Jean-Paul Larbre^{2,12} , Guillaume Sarrabay¹³ , Flora Magnotti¹ , Gillian I. Rice¹⁴ , Françoise Bleicher¹⁵ , Jonathan Reboulet¹⁵ , Samir Merabet¹⁵ , Thomas Henry¹ , Yanick J. Crow^{4,16} , Mathias Faure¹ , Thierry Walzer^{1,2} , and Alexandre Belot^{1,2,6} 

Juvenile idiopathic arthritis is the most common chronic rheumatic disease in children, and its etiology remains poorly understood. Here, we explored four families with early-onset arthritis carrying homozygous loss-of-expression mutations in *LACC1*. To understand the link between *LACC1* and inflammation, we performed a functional study of *LACC1* in human immune cells. We showed that *LACC1* was primarily expressed in macrophages upon mTOR signaling. We found that *LACC1* deficiency had no obvious impact on inflammasome activation, type I interferon response, or NF-κB regulation. Using bimolecular fluorescence complementation and biochemical assays, we showed that autophagy-inducing proteins, RACK1 and AMPK, interacted with *LACC1*. Autophagy blockade in macrophages was associated with *LACC1* cleavage and degradation. Moreover, *LACC1* deficiency reduced autophagy flux in primary macrophages. This was associated with a defect in the accumulation of lipid droplets and mitochondrial respiration, suggesting that *LACC1*-dependent autophagy fuels macrophage bioenergetics metabolism. Altogether, *LACC1* deficiency defines a novel form of genetically inherited juvenile arthritis associated with impaired autophagy in macrophages.

Introduction

Autoinflammatory diseases are innate immunological disorders associated with sterile inflammation in the absence of auto-antibodies or autoreactive T cells (Manthiram et al., 2017). This group includes a series of inherited diseases affecting specific inflammatory pathways. Inflammasomes are highly regulated multi-protein complexes that can detect various danger signals and cleave precursors of IL-1β and IL-18 pro-inflammatory

cytokines. Inflammasomopathies are due to genetic defects driving deregulated maturation and secretion of these cytokines (Harapas et al., 2018). Type-I interferonopathies are a group of diseases characterized by an excessive secretion or signaling of type-I IFN (IFN-I), which results in the up-regulation of IFN-stimulated genes (i.e., IFN signature; Rodero and Crow, 2016; Rice et al., 2013). NF-κB is a transcription factor involved in the

¹Centre International de Recherche en Infectiologie/International Center for Infectiology Research, Institut National de la Santé et de la Recherche Médicale, U1111, Ecole Normale Supérieure de Lyon, Université Lyon 1, Centre National de la Recherche Scientifique, UMR5308, Lyon, France; ²National Reference Centre for Rheumatic and Autoimmune Diseases in Children, RAISE, Paris and Lyon, France; ³General Pediatrics, Infectious Disease and Internal Medicine Department, Hôpital Robert Debre, Assistance Publique-Hôpitaux de Paris, Paris, France; ⁴Laboratory of Neurogenetics and Neuroinflammation, Paris Descartes-Sorbonne Paris Cité University, Institut Imagine, Hôpital Necker, Paris, France; ⁵Internal Medicine, Croix Rousse Hospital, Hospices Civils de Lyon, Lyon, France; ⁶Pediatric Nephrology, Rheumatology, Dermatology Department, Hôpital Femme Mère Enfant, Hospices Civils de Lyon, Bron, France; ⁷Pediatric Pneumology, Immunology and Intensive Care Medicine, Charité University Medicine Berlin, German Rheumatism Research Center, Leibniz Association, Berlin Institute of Health, Berlin, Germany; ⁸Department of Molecular Biology and Genetics, Faculty of Science and Letters, Istanbul Technical University, Istanbul, Turkey; ⁹Molecular Development of the Immune System Section, Laboratory of Immune System Biology, National Institute of Allergy and Infectious Diseases, National Institutes of Health, Bethesda, MD; ¹⁰Immunology Department, Hôpital Edouard Herriot, Hospices Civils de Lyon, Lyon, France; ¹¹Immunology Department, Hospices Civils de Lyon, Centre Hospitalier Lyon Sud, Pierre-Bénite, France; ¹²Rheumatology Unit, Hospices Civils de Lyon, Centre Hospitalier Lyon Sud, Pierre-Bénite, France; ¹³Centre Hospitalier Universitaire Montpellier, University of Montpellier, Laboratory of Rare and Autoinflammatory Genetic Diseases and Centre de Référence des Maladies Auto-Inflammatoires et des Amyloses d'Origine Inflammatoire, Montpellier, France; ¹⁴Division of Evolution and Genomic Sciences, School of Biological Sciences, Faculty of Biology, Medicine and Health, University of Manchester, Manchester, UK; ¹⁵Institut de Génétique Fonctionnelle de Lyon, Université de Lyon, Université Lyon 1, Centre National de la Recherche Scientifique, Ecole Normale Supérieure de Lyon, Lyon, France; ¹⁶Centre for Genomic and Experimental Medicine, Medical Research Council Institute of Genetics and Molecular Medicine, University of Edinburgh, Edinburgh, UK; ¹⁷Assistance Publique-Hôpitaux de Paris, Hôpital Tenon, Sorbonne Université, Service de Médecine Interne, Centre de Référence des Maladies Auto-Inflammatoires et des Amyloses d'Origine Inflammatoire, Paris, France; ¹⁸Assistance Publique-Hôpitaux de Paris, Hôpital Trousseau, Université Pierre-et-Marie-Curie-Paris 6, Institut National de la Santé et de la Recherche Médicale UMRS 933, Paris, France.

Correspondence to Alexandre Belot: alexandre.belot@chu-lyon.fr; Thierry Walzer: Thierry.walzer@inserm.fr.

© 2021 Omarjee et al. This article is distributed under the terms of an Attribution-Noncommercial-Share Alike-No Mirror Sites license for the first six months after the publication date (see <http://www.rupress.org/terms/>). After six months it is available under a Creative Commons License (Attribution-Noncommercial-Share Alike 4.0 International license, as described at <https://creativecommons.org/licenses/by-nc-sa/4.0/>).

induction of numerous pro-inflammatory cytokines, downstream of several innate immune receptors. NF- κ B activation is tightly regulated through multiple post-translational mechanisms, including ubiquitination (Aksentijevich and Zhou, 2017). Genetic disorders leading to NF- κ B overactivation are reported as NF- κ B-related autoinflammatory diseases (relopathies; Steiner et al., 2018).

Beyond these well-described groups of diseases, several forms of autoinflammation remain unclassified. Juvenile idiopathic arthritis (JIA) is a heterogeneous inflammatory disease affecting joints of children <16 yr (Prakken et al., 2011). Mechanisms of joint inflammation remain poorly understood in the context of juvenile arthritis. The main features of this type of inflammation include (1) hypervascularization and hyperplasia of the synovial membrane and infiltration of inflammatory monocytes, T helper type 1 (Th1) and Th17 cells, in the synovial fluid with accumulation of macrophages in the synovial membrane (Evans et al., 2009; Dennis et al., 2014); (2) presence of inflammatory cytokines and metabolites in the synovial fluid; and (3) cartilage and bone erosion by matrix metalloproteases and osteoclasts (Firestein and McInnes, 2017). Early genetic investigations in JIA through genome-wide association studies identified the HLA system and genes involved in lymphocyte regulation as important (Hersh and Prahalad, 2015). More recently, next-generation sequencing applied to familial forms of JIA identified LACC1 mutations as the first model of autosomal recessive juvenile polyarthritis (Kallinich et al., 2016; Karacan et al., 2018; Rabionet et al., 2019; Wakil et al., 2015). These patients were negative for autoantibodies, including antinuclear antibodies, and the first patients reported displayed features of systemic JIA, suggesting dysregulation of innate immunity.

LACC1, also known as C13ORF31 or FAMIN, is a 47-kD protein expressed in myeloid cells (Cader et al., 2016; Lahiri et al., 2017; Skon-Hegg et al., 2019). Genome-wide association studies had previously associated LACC1 to immune- and bacteria-mediated diseases such as inflammatory bowel diseases and leprosy. Mouse and human studies have suggested multiple roles of LACC1 in fatty acid synthase-mediated de novo lipogenesis (Cader et al., 2016), NOD2-mediated signaling (Lahiri et al., 2017), ER stress (Huang et al., 2019), and, more recently, purine nucleotide cycle (Cader et al., 2020). A common finding in these studies was an impairment of macrophage effector function in terms of production of cytokines and reactive oxygen species in the absence of LACC1, consistent with aberrant host microbial interactions. However, these studies did not provide solid evidence to explain autoinflammation in patients. Moreover, there are conflicting data in terms of LACC1 function, Laccase domain activity (active or inactive; Cader et al., 2016; Lahiri et al., 2017), and subcellular localization (peroxisome, cytoplasm, mitochondria; Cader et al., 2016; Lahiri et al., 2017). Of note, *Lacc1*-deficient mice do not develop spontaneous arthritis, questioning the use of this model to understand human pathology.

Genetic variation at the *LACC1* locus has been reported to affect the risk of Crohn's disease (Umeno et al., 2011). This is also the case for several variants of modulators of autophagy, including *NOD2* and *ATG16L1* variants (Assadi et al., 2016; Baldassano et al., 2007; Philpott et al., 2014; Sales-Marques

et al., 2014). Autophagy is an evolutionarily conserved mechanism essential in cellular detoxification and metabolism through the lysosomal degradation pathway (Levine and Kroemer, 2019). Autophagy is regulated by upstream energy sensors such as mammalian target of rapamycin (mTOR) and AMP-activated protein kinase (AMPK), which control anabolic and catabolic programs, respectively. mTOR inhibits autophagy at transcriptional (TFEB) and post-translational (phosphorylation of ULK complex) levels, while AMPK activation results in ULK complex activation and mTOR inhibition. Following the initiation of autophagy, leading to de novo formation of an isolated membrane called the phagophore, the two ubiquitin-like conjugation systems, ATG5-ATG12 and ATG8/LC3, concur to mediate the elongation of both extremities of the phagophore. During this process, a lipidated form of the otherwise cytosolic ATG8/LC3 protein (referred to as LC3-I) is incorporated within the growing autophagosome surrounding cellular cargos, and is a key marker of this vesicular structure (referred to as LC3-II). Ultimately, autophagosomes, which sequester cytosolic material, mature to fuse with lysosomes, leading to the degradation and the recycling of the complete intracellular content. In murine cell lines and rat hepatocytes, autophagy regulates lipid metabolism (Nguyen et al., 2017; Singh et al., 2009) and mitochondria turnover. During bacterial infection, the NOD2-ATG16L1 complex recruits autophagy machinery for pathogen uptake and elimination (Homer et al., 2010; Travassos et al., 2010). *ATG16L1*-deficient macrophages secrete higher levels of IL-1 β (Saitoh et al., 2008), as do macrophages treated with autophagy maturation inhibitor bafilomycin A1 (BafA1; Harris et al., 2011). Moreover, knockdown of two important proteins of the autophagy mechanism, *ATG16L1* and *IRGM*, in human dendritic cells stabilizes their interaction with T cells, thereby favoring inflammatory Th17 T cell activation (Wildenberg et al., 2012). Enhanced Th17 responses were also observed in *LACC1* knockout arthritis mouse models (Skon-Hegg et al., 2019).

In this study, we report the identification of loss-of-function *LACC1* mutations in patients from four unrelated families, and study the role of *LACC1* in human immune cells. Our functional analyses using different assays do not support a link between *LACC1* and previously reported pathways involved in autoinflammation, i.e., inflammasome, regulation of NF- κ B, or IFN-I. We found that *LACC1* was primarily expressed in macrophages. Using an unbiased proteomic screen and various biochemical and functional systems, we show that *LACC1* is a novel component of the autophagy machinery operating in macrophages downstream of the energy sensor AMPK. Moreover, *LACC1* is essential to promote the accumulation of lipid droplets in macrophages, which fuels mitochondrial respiration via fatty acids. Thus, *LACC1* loss of function defines a novel form of inflammation associated with defects in macrophage autophagy and metabolism.

Results

Next-generation sequencing of JIA patients identifies homozygous loss-of-function mutations in *LACC1*

Four consanguineous families of North African (A), Lebanese (B), Turkish (C), and African (D) ancestry were identified with

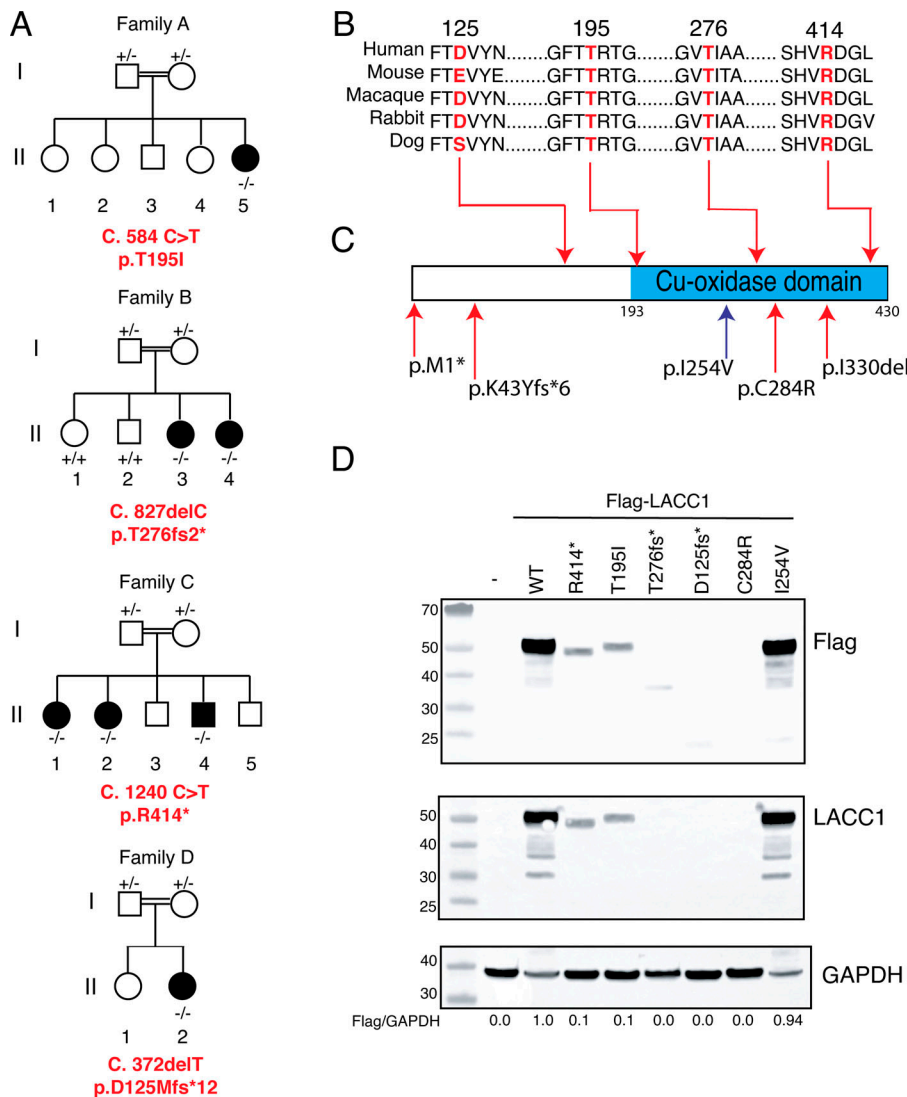


Figure 1. Whole or targeted exome sequencing identifies loss-of-function mutations in LACC1 from JIA families. (A) Pedigree of four JIA families with identified LACC1 mutations. (B) Protein alignment at mutated amino acid sites across species. (C) Representation of novel JIA mutations (upper red arrows), previously reported JIA mutations (lower red arrow), and Crohn's disease-associated variant (lower blue arrow) on the structure of LACC1 with a predicted copper-oxidase domain. (D) Immunoblots of 293T cells transfected with plasmids encoding for flagged forms of LACC1 WT or variants (representative of two experiments).

polyarticular JIA (pJIA, Fig. 1 A and Table 1). Patient A.II.5 was diagnosed with pJIA at the age of 5 mo and was initially treated with corticosteroids. Anti-IL-1 therapy was then administered to treat the systemic symptoms with a partial response. This patient is now 11 yr old and treated with anti-IL-6 antibodies, with good efficacy. The clinical cases of patients B.II.3 and 4 have already been reported (Kallinich et al., 2016). Both developed severe pJIA at the age of 16 mo and 15 mo, respectively, and a LACC1 mutation was identified. Of note, patient B.II.3 received bone marrow transplantation for precursor-B acute lymphoblastic leukemia that cured arthritis, suggesting that hematopoietic cells mediate LACC1-related arthritis. Finally, patients C.II.1, C.II.2, and C.II.4 were diagnosed with pJIA, which started at the age of 11 mo and 5 yr for C.II.2 and C.II.4, respectively. The two girls showed poor response to anti-TNF and anti-IL-1 therapy, while anti-TNF therapy was effective in C.II.4. Finally, patient D.II was diagnosed with pJIA at the age of 2 yr and is currently under tocilizumab therapy. Table 1 summarizes previous (in italics) and current therapies (bold) administered to each patient. Importantly, neither rheumatoid factor nor anti-

citrullinated peptide antibodies were identified in patients from families A, B, C, or D.

Whole-exome (families B and C) or panel-exome sequencing (families A and D) was performed and identified homozygous mutations in LACC1 (Fig. 1 A) leading to amino acid substitution (family A) or stop codon insertion (families B, C, and D). All affected regions of LACC1 protein were highly conserved during evolution (Fig. 1 B), and in silico combined annotation-dependent depletion and population frequency (Genome Aggregation Database) analysis predicted rare damaging variants with scoring of 22.6 and 42 in families B and C, respectively. Interestingly, the position of LACC1 variants (including previously reported ones) was mostly concentrated in the C-terminal Laccase domain (Fig. 1 C). To determine the impact of those predicted highly damaging variants on LACC1 expression, we expressed their tagged forms including the p.C284R (systemic JIA) and p.I254 (Crohn's) LACC1 variants in 293T cells. Western blot (WB) analysis of cell lysates demonstrated a loss of >90% of the total amount of LACC1 for all JIA variants, while the Crohn's variant p.I254V did not impact the level of protein expression

Table 1. **Clinical and biological characteristics of the JIA patients**

Family Patient	A	B		C			D
	II.5	II.3	II.4	II.1	II.2	II.4	II
Age (yr)	11	11	10	23	18	9	5
Ethnicity	African	Lebanese		Turkish			African
Consanguinity	Yes	Yes		Yes			Yes
LACC1 mutation	Homozygous c. 584 C>T p.T195I	Homozygous c. 827delC p.T276fs*2		Homozygous c.1240 C>T p.R414*			Homozygous c.372delT p.D125Mfs*12
CADD	NA	22.6		42			NA
GNOMAD	0	0		0			0
Disease	Severe pJIA	Severe pJIA		pJIA			Severe pJIA
Autoimmune characteristics	No antinuclear antibodies, no rheumatoid factors, no anti-cyclic citrullinated peptide						
Lymphocytes (1,400–3,700/ μ l)	1,410	NA	NA	1,213	1,395	3,600	5,000
CD4 T cells (530–1,500/ μ l)	NA	NA	NA	607	525	1285	NA
CD8 T cells (330–1,100/ μ l)	NA	NA	NA	309	455	708	NA
CD19 B cells (110–860/ μ l)	NA	NA	NA	NA	214	925	NA
NK cells (100–480/ μ l)	NA	NA	NA	NA	177	412	NA
Sera Ig							
IgG (4–15 g/liter)	8.1	NA	5.3	3.4	10.3	8.1	3.6
IgA (0.78–4.110.7 g/liter)	0.54	NA	0.61	0.57	1.41	0.57	0.26
IgM (0.9 g/liter)	0.63	NA	0.26	0.64	0.31	0.77	0.19
IgE (<12150 kU/liter)	438	NA	6.4	16.4	2	178	75.6
Age of onset	5 mo	16 mo	15 mo	12 mo	11 mo	4 yr	2 yr
Associated uveitis	No						
Treatments	Corticosteroids	<i>Etanercept</i>	Adalimumab	<i>Etanercept</i>	Etanercept	Corticosteroids	
	<i>Anakinra</i>	<i>Anakinra</i>	<i>Hydroxychloroquine</i>	<i>Anakinra</i>		<i>Methotrexate</i>	
	<i>Canakinumab</i>	<i>Tocilizumab</i>		<i>Secukinumab</i>		<i>Enbrel</i>	
	Tocilizumab	BMT		<i>Tocilizumab</i> , Baricitinib		Tocilizumab	
	Methotrexate						

Text in italics indicates previous therapies; text in bold indicates current therapies. BMT, bone marrow transplant; CADD, combined annotation-dependent depletion; GNOMAD, Genome Aggregation Database; NA, not available; NK, natural killer cells.

(Fig. 1 D). This demonstrates that LACC1 mutations in JIA patients induce a lower expression of LACC1.

LACC1 expression is induced by M-CSF during differentiation of monocyte-derived macrophages, in an mTOR-dependent pathway

LACC1 expression has been reported in murine macrophages and neutrophils (Cader et al., 2016; Skon-Hegg et al., 2019), but limited explorations have been performed in human cells (Lahiri et al., 2017). The protein database BioGPS indicated highest LACC1 mRNA levels in human macrophages (<http://biogps.org/#goto=genereport&id=144811>). To screen for LACC1 expression at the protein level, we searched for a specific antibody to detect endogenous levels of LACC1 expressed by the monocytic U937 cell line differentiated or not in macrophages. We also used U937 cells in which we either knocked out or endogenously tagged (in

frame) LACC1 by CRISPR/Cas9 genome editing as a control. Numerous commercial antibodies were tested by WB, including those that were used in previous articles on LACC1. Only one of them (clone E7; Santa Cruz) showed a specific staining by WB (Fig. S1 A). We then measured LACC1 expression in different primary human blood cells using this specific antibody. LACC1 expression was undetectable in lymphocytes and monocytes (Fig. 2 A) but was strongly induced in macrophages differentiated from monocytes with M-CSF. LACC1 was also expressed in GM-CSF-derived macrophages and GM-CSF/IL-4-derived dendritic cells, albeit at lower levels than in M-CSF-derived macrophages (hereafter simplified as macrophages; Fig. 2 B). Interestingly, macrophages also expressed a short form of LACC1 (Fig. 2, A and B) that may correspond to a cleavage product of the protein. LACC1 expression was rapidly induced by M-CSF during macrophage differentiation from day

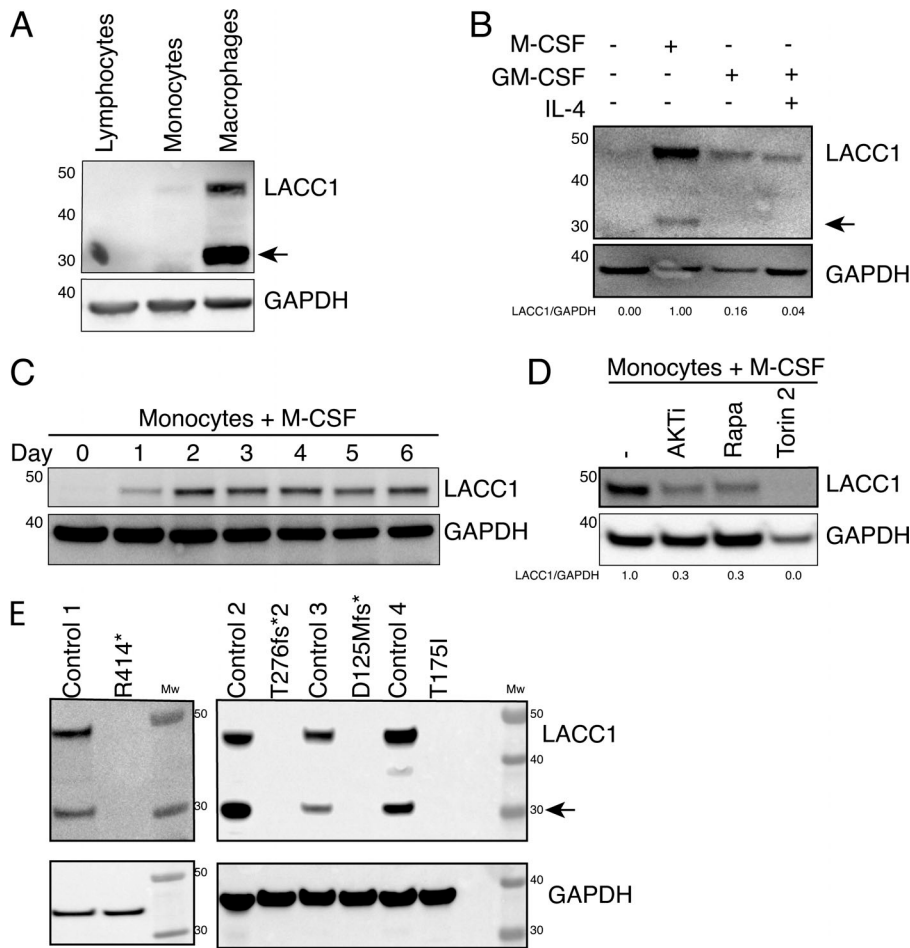


Figure 2. LACC1 is strongly expressed in an mTOR-dependent manner during M-CSF-induced human monocyte-macrophage differentiation. (A) Immunoblots of various immune cells isolated from buffy coat (lymphocyte and monocytes) or differentiated in vitro (M-CSF macrophages; representative of three experiments). Arrowhead indicates short fragment of LACC1. (B) Immunoblot of monocytes stimulated with the indicated cytokines for 6 d (representative of two experiments). Arrowhead indicates short fragment of LACC1. (C) Immunoblots of monocytes treated with M-CSF at different time points (representative of three experiments). (D) Immunoblots of monocytes treated with M-CSF and inhibitors (AKTi, Rapamycin, and Torin2) over 24 h (representative of two experiments). (E) Immunoblots of macrophages derived from either four healthy donors or four JIA patients bearing indicated mutations in LACC1. Mw, molecular weight. For B and D, a quantification of LACC1 level is shown below the blot.

1 onwards (Fig. 2 C). We used various pharmacological inhibitors to identify signaling pathways regulating LACC1 induction upon M-CSF stimulation. p38, JNK, ERK, and Pi3K pathways did not contribute to this induction (Fig. S2). Conversely, inhibitors targeting the protein kinase B (PKB, also known as AKT)-mTOR pathway suppressed LACC1 expression (Fig. 2 D and Fig. S2). These results point the M-CSF-AKT-mTOR axis as an essential pathway for LACC1 expression during macrophage differentiation. Next, we measured LACC1 expression in patient-derived macrophages and observed a total absence of the protein, confirming that these point mutations induced complete deficiency of LACC1 at the endogenous level (Fig. 2 E).

LACC1 deficiency does not influence inflammasome, IFN-I, or NF-κB activation

Aberrant activation of the IFN-I pathway, NF-κB-mediated signaling, or inflammasome complex may lead to different forms of auto-inflammatory diseases (Fig. 3 A). As some of the features observed in these conditions overlap with those of JIA patients (notably fever, arthritis, C-reactive protein [CRP] increase, and elevated inflammatory blood markers; Fig. S3 A), we looked for evidence of a link between LACC1 and such autoinflammatory pathways. The expression of IFN-stimulated genes (ISGs) was measured on three patients' whole blood samples from one family, and an IFN score was calculated as previously described

(Pescarmona et al., 2019). The IFN score was similar between LACC1 patients and healthy donors, well below that of patients affected by Aicardi-Goutières syndrome (AGS) and stimulator of IFN genes (STING)-associated vasculopathy of infancy (SAVI), two inherited interferonopathies (Fig. 3 B). To test whether the loss of LACC1 favored excessive activation of the inflammatory NF-κB pathway, we knocked down LACC1 expression in primary macrophages using siRNA (hereafter called as siLACC1 macrophages), and measured IKβα expression, IKKβ phosphorylation, and cytokine secretion in response to heat-killed bacteria (*Salmonella enterica* serovar Typhimurium and *Staphylococcus aureus*) or LPS, a bacterial cell wall component. Similar degradation of IKβα, phosphorylation of IKKβ, and TNF secretion were observed in response to treatments in control and siLACC1 macrophages (Fig. 3, C and D). Patients' macrophages also produced normal levels of TNF in response to LPS (Fig. 3 E), and CRISPR/Cas9-mediated knockout of LACC1 did not influence the capacity of U937 cells differentiated into macrophages to produce TNF upon LPS stimulation (Fig. S3 B). IL-1β release following inflammasome activation requires both a priming signal and an activating signal. In cryopyrinopathies, the priming signal is sufficient to activate inflammasome and subsequent IL-1β/IL-18 release, while other inflammasomopathies result in higher secretion of cytokines upon administration of both signals (Carta et al., 2015; Tassi et al., 2010). This was not observed in patients'

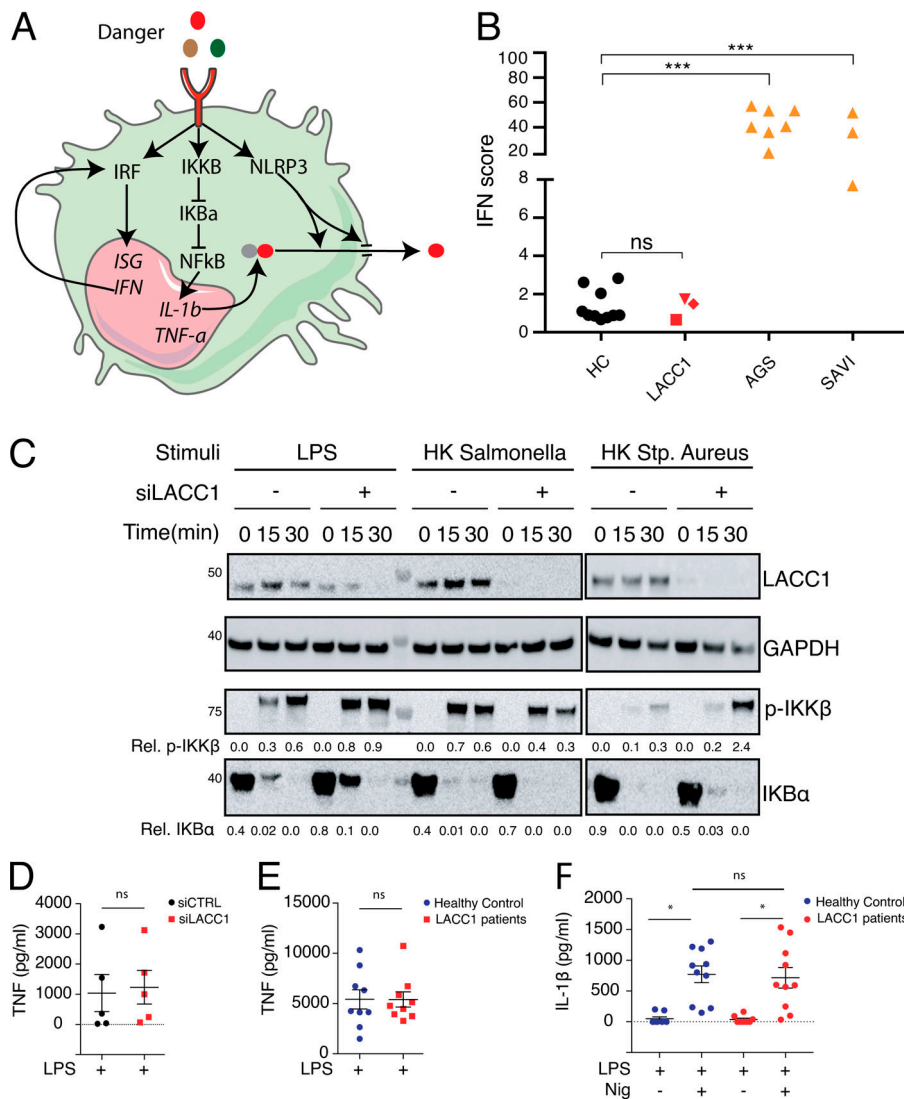


Figure 3. LACC1 deficiency does not seem to be connected to known monogenic auto-inflammatory pathways. (A) Illustration of IFN, NF-κB, and inflammasome activation pathways. IRF, IFN regulatory factor. (B) IFN score determined from Nanostring measurement of ISGs in whole blood of 10 controls and patients C.II.1, C.II.2, and C.II.4. Samples from Aicardi-Goutières syndrome (AGS) and STING-associated vasculopathy of infancy patients (SAVI) were used as controls. ***, $P < 0.0005$ (unpaired t test). (C) Immunoblots (IB) of indicated siRNA-transfected human monocyte-derived macrophages stimulated with LPS ($n = 3$), heat-killed (HK) *Salmonella*, or heat-killed *S. (Stp.) aureus* ($n = 2$) for 15 and 30 min. (D) TNF secretion of human monocyte-derived macrophages stimulated with LPS for 3 h ($n = 4$). (E) TNF secretion of monocyte-derived macrophages obtained from healthy donors and LACC1 patients stimulated with LPS for 3 h ($n = 9$). (F) IL-1β secretion of monocyte-derived macrophages obtained from healthy donors and LACC1 patients stimulated with LPS ± nigericine (Nig; $n = 10$). *, $P < 0.05$ (paired t test).

macrophages primed with LPS alone or with both signals (Fig. 3 F). A similar conclusion was reached using U937 cells (Fig. S3 C). Altogether, these functional tests do not support a role for LACC1 in the regulation of inflammasome activation, IFN-I signaling, or NF-κB activation.

A proteomic screen identifies autophagy-associated proteins as LACC1 partners

Roles for LACC1 were previously demonstrated in lipid metabolism, NOD2-mediated NF-κB signaling, ER stress, and in the purine nucleotide cycle (Cader et al., 2016; Lahiri et al., 2017; Huang et al., 2019). In an attempt to understand how LACC1 acted at the molecular level, we performed a bimolecular fluorescence complementation screen to identify interacting partners of LACC1. This screen consisted of coexpressing LACC1 fused with the N-terminal fragment of the Venus fluorescent protein and a library of 6,973 open reading frames (ORFs) fused with the complementary C-terminal fragment of Cerulean in HEK293T (Grinberg et al., 2004; Fig. 4 A). Potential molecular interactions led to Venus reconstitution and fluorescence emission, enabling cell sorting by flow cytometry (Fig. 4 B).

4,308 cloned ORFs from Venus⁺ cells were sequenced and filtered so as to select the highest enriched ORFs in Venus⁺ cells but depleted in Venus⁻ cells. This resulted in the identification of 28 putative LACC1 interactors (Table 2), which included SDHAF4, a cofactor of succinate dehydrogenase complex, subunit A (SDHA) previously reported to interact with LACC1 (Lahiri et al., 2017). Interestingly, among the other proteins identified, two of them, RACK1 and especially AMPK (encoded by RACK1 and PRKAA1) are key regulators of autophagy induction (Zhao et al., 2015; Erbil et al., 2016), and several others have a known connection with autophagy (VEGF, TPK1, SUV39H1, CORO1C; Spengler et al., 2020; Miao et al., 2019; Kannan et al., 2017; Schmelzle et al., 2004). Through coimmunoprecipitation assays in 293T cells, we confirmed the interaction of LACC1 with AMPK and RACK1 (Fig. 4 C). Moreover, we also confirmed the interaction between endogenous LACC1 and RACK1 by immunoprecipitation of RACK1 followed by LACC1 WB in macrophages (Fig. 4 D). Monocytes were used as a negative control in this experiment as they do not express LACC1. This led to the identification of AMPK and RACK1 as novel partners of LACC1 in human macrophages.

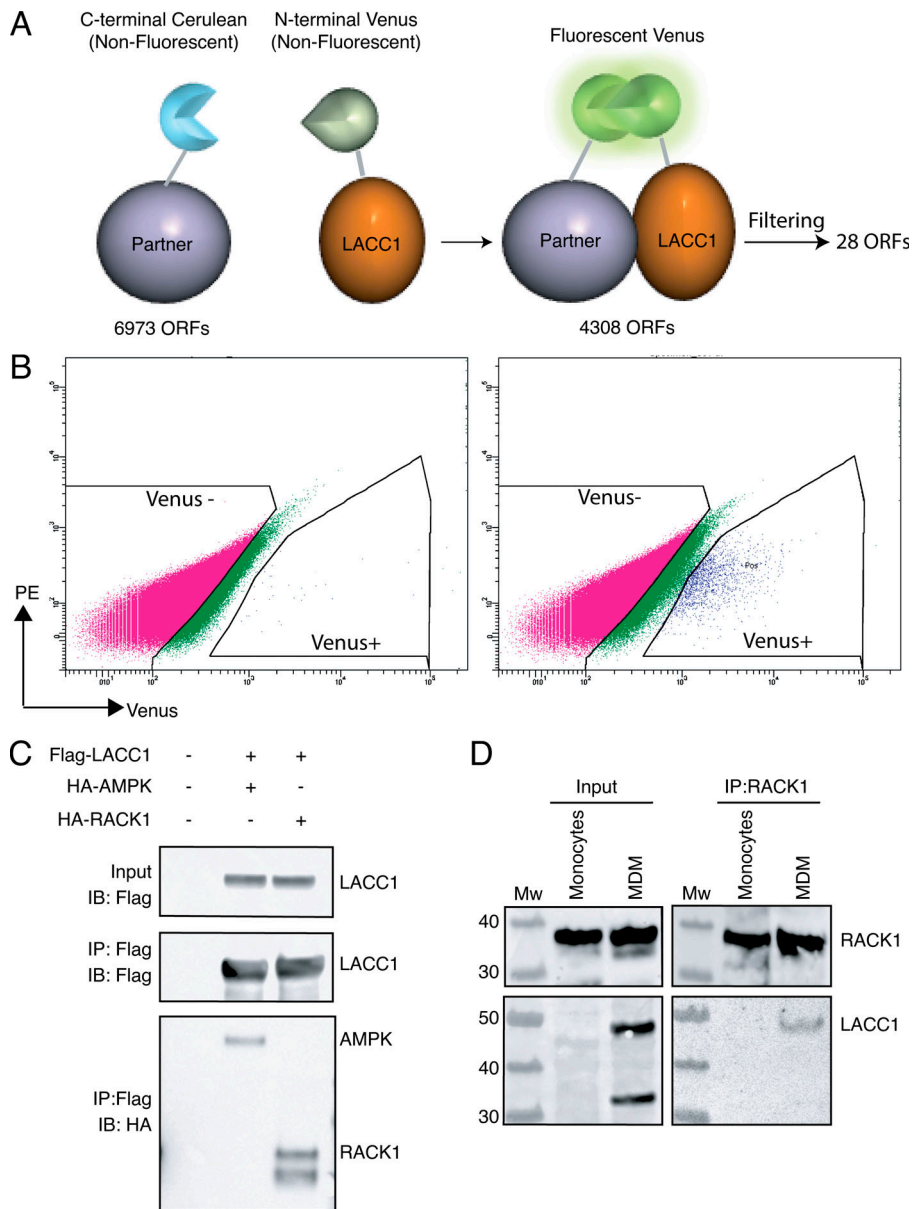


Figure 4. A large-scale proteomic screen identifies AMPK and RACK1 as LACC1 partners. (A) Schematic representation of proteomic screen design consisting of the cotransfection of LACC1 and ORF library tagged with either fragments of Venus protein. (B) GFP-positive cell sorting of 293T cells expressing BIFC ORFs transfected with (right) or without (left) N-Venus-LACC1. (C) Immunoblots of Flag-immunoprecipitated cell lysates of 293T cells cotransfected with tagged LACC1, AMPK, or RACK1 expression vectors (representative of three experiments). (D) Immunoblots of endogenous RACK1-immunoprecipitated cell lysates of human monocytes and macrophages. Input, immunoprecipitated (IP) fractions were immunoblotted against LACC1 (representative of two experiments). MDM, monocyte-derived macrophage; Mw, molecular weight.

LACC1 promotes autophagic flux in macrophages

Having established the interaction between LACC1, AMPK, and RACK1, we sought to investigate the link between LACC1 and autophagy. We treated macrophages with inhibitors of late autophagic stages, involving lysosomal degradation. We used BafA1, inhibiting the fusion of lysosomes with autophagosomes; chloroquine, a potent inhibitor of autophagolysosome acidification; or the lysosomal cathepsin inhibitors E64D or pepstatin A. These different treatments resulted in the rapid (1 h) accumulation of full-length LACC1 and the disappearance of the 30-kD cleavage product (Fig. S4 A).

To test the role of LACC1 in autophagy, we first treated control or patient macrophages (carrying biallelic p.D125fs*, p.T195I, and T276fs* variants) with BafA1 and measured the level of expression of LC3-II, which is normally degraded during the autophagy process, but accumulates when the autophagy maturation step is compromised. Upon BafA1 treatment, LC3-II

accumulated in both control and patient macrophages, albeit to a lower extent in LACC1-deficient patients (Fig. 5 A). Due to the varying autophagy flux among healthy donors (Fig. 5 A) arising from different genetic backgrounds, we reasoned that LACC1 knockdown with siRNA in the same donor macrophages would overcome this genetic disparity. We therefore compared autophagy flux between control and siLACC1 macrophages treated with BafA1 at different time points, and measured the level of LC3-II accumulation. The inhibition of the autophagosome-lysosome fusion upon BafA1 treatment resulted in an expected and a rapid accumulation of LC3-II in control macrophages but not as much in LACC1 knocked-down macrophages (Fig. 5 A), suggesting that LACC1 is required for optimal macrophage autophagy. Similar defects in autophagy were observed in siLACC1 macrophages when they were treated with chloroquine and rapamycin (Fig. S4, B and C). To further substantiate the link between LACC1 and autophagy, we transfected LACC1 in the

Table 2. List of interactors derived from proteomic assay

ORF	Numbers of reads per ORF			Frequency of reads per ORF			ORF enrichment
	Pre-sorted cells	GFP ⁺ cells	GFP ⁻ cells	Pre-sorted cells	GFP ⁺ cells	GFP ⁻ cells	
SDHAF4	154	5,994	0	1.309E-03	3.734E-02	0	28.52
VEGF	107	3,215	0	9.097E-04	2.003E-02	0	22.02
IL18BP	161	4,143	0	1.369E-03	2.581E-02	0	18.85
KRT17	159	3,943	0	1.352E-03	2.456E-02	0	18.17
PPAP2A	112	2,509	0	9.522E-04	1.563E-02	0	16.41
TPK1	135	2,252	0	1.148E-03	1.403E-02	0	12.22
RNPS1	199	3,112	0	1.692E-03	1.939E-02	0	11.46
OSBPL2	294	4,415	0	2.499E-03	2.750E-02	0	11.00
CD160	104	1,492	0	8.842E-04	9.294E-03	0	10.51
RACK1	235	2,699	0	1.998E-03	1.681E-02	0	8.42
CDV1	165	1,719	0	1.403E-03	1.071E-02	0	7.63
ADAMTS18	379	3,785	0	3.222E-03	2.358E-02	0	7.32
NY-REN-7	134	723	0	1.139E-03	4.504E-03	0	3.95
SORD	122	594	0	1.037E-03	3.700E-03	0	3.57
ZNF444	120	571	0	1.020E-03	3.557E-03	0	3.49
POLD2	619	2,684	0	5.263E-03	1.672E-02	0	3.18
SUV39H1	279	1,106	0	2.372E-03	6.890E-03	0	2.90
ACOT9	801	3,068	0	6.810E-03	1.911E-02	0	2.81
GCAT	209	781	0	1.777E-03	4.865E-03	0	2.74
PCYOX1	149	445	0	1.267E-03	2.772E-03	0	2.19
CORO1C	597	1,712	0	5.075E-03	1.066E-02	0	2.10
FBXO42	150	353	0	1.275E-03	2.199E-03	0	1.72
C1orf73	492	1,097	0	4.183E-03	6.833E-03	0	1.63
PRKAA1	105	211	0	8.927E-04	1.314E-03	0	1.47
LILRA3	581	1,074	0	4.939E-03	6.690E-03	0	1.35
MRPL21	174	274	0	1.479E-03	1.707E-03	0	1.15
ANKRA2	448	694	0	3.809E-03	4.323E-03	0	1.14
RBM30	230	339	0	1.955E-03	2.112E-03	0	1.08

autophagy reporter cell line HeLa GFP-LC3 (Klionsky et al., 2008; Mizushima et al., 2010). Upon transfection, we noticed a trend to increased GFP dots corresponding to LC3-coated autophagosomes in LACC1-transfected cells compared with controls (Fig. S4 D), suggesting that LACC1 overexpression promotes autophagy.

To confirm the involvement of LACC1 in autophagy, we then compared the consequences of knocking down either LACC1 or ATG5, an essential protein for the elongation of growing autophagosomes in various autophagy-modulating conditions. Macrophages were cultured in normal or HBSS starvation medium (a condition of AMPK-dependent autophagy induction) and treated with BafA1 to visualize autophagy upstream signaling and flux. Results in Fig. 5 C show a comparable deficit in the accumulation of LC3-II and p62 (a natural cargo of ongoing autophagy) in LACC1 and ATG5 knocked-down macrophages. AMPK phosphorylation was induced by starvation, and this

phosphorylation was identical in LACC1 and ATG5 knocked-down macrophages, thereby indicating that LACC1 acts downstream of AMPK in the autophagy cascade. mTOR activity, antagonistic to AMPK and autophagy, was assessed by measuring ribosomal S6 protein and 4-EBP1 phosphorylation levels. Strikingly, both proteins were highly phosphorylated in both ATG5 and LACC1 knockdown conditions, pointing toward spontaneous up-regulation of mTOR signaling. This phenomenon could arise through compensatory mechanisms to failed LACC1-mediated autophagy flux. Altogether, these results establish that LACC1 is important to promote autophagic flux in macrophages downstream of AMPK.

Loss of LACC1 impairs lipid droplet-fueled mitochondrial respiration and phagocytosis

LACC1-deficient macrophages were previously reported to have decreased fatty acid pools and impaired cell metabolism due to

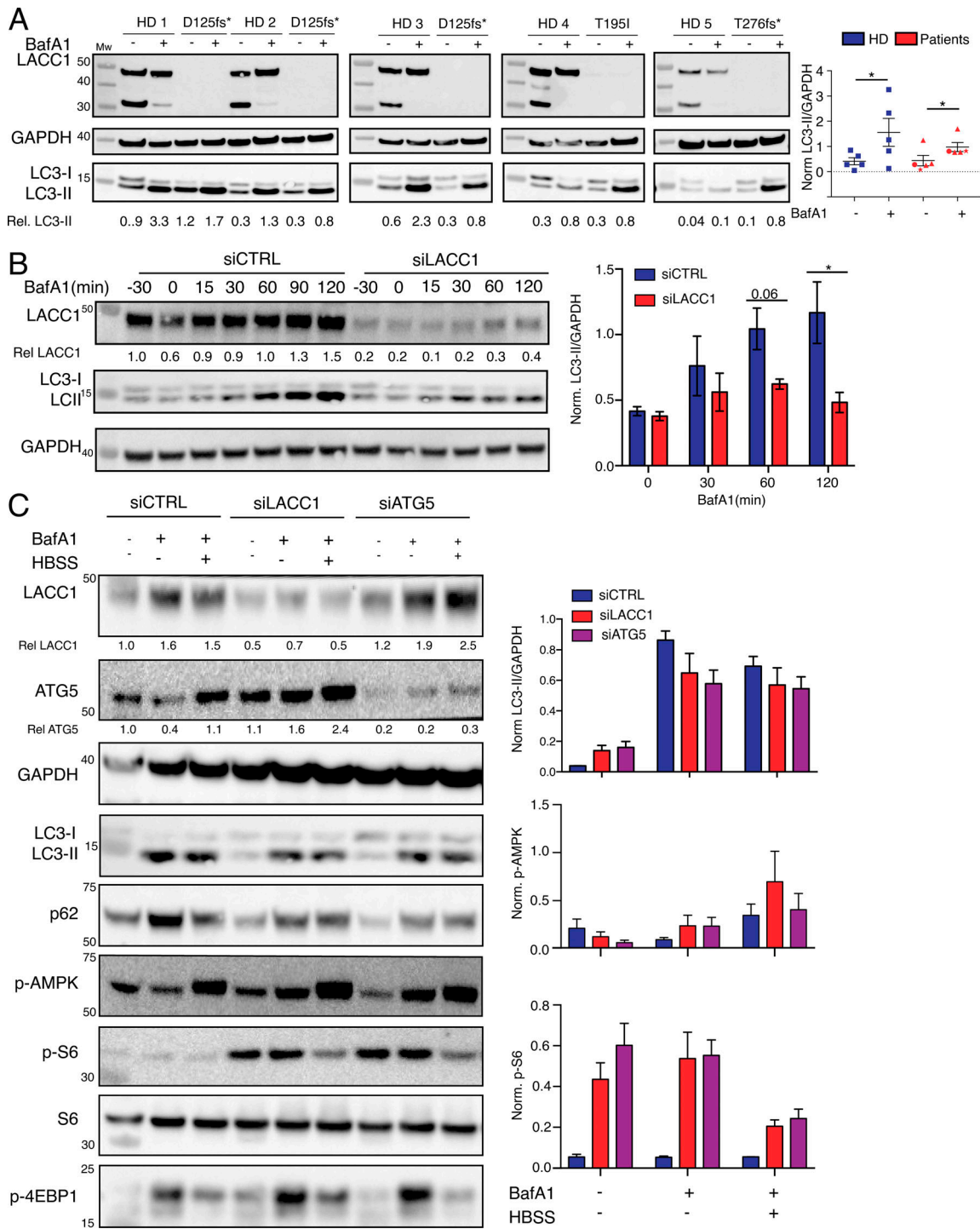


Figure 5. **LACC1 regulates autophagy and associated signaling.** (A) Immunoblot of five healthy donors (HD) versus five patients (three different samplings of D125fs* [triangle], T196I [circle], and T276fs* [star]) macrophages treated with BafA1 for 2 h. Right: LC3-II levels normalized to GAPDH. (*, $P < 0.05$ [paired t test]). (B) Immunoblot of control versus siLACC1 macrophages treated with BafA1 at different time points (representative of three experiments). Right: Accumulation of LC3-II levels normalized to GAPDH at selected time points based on the immunoblots. *, $P < 0.05$ (paired t test). (C) Immunoblot of control versus LACC1-deficient macrophages treated with BafA1 in RPMI or HBSS starvation medium for 2 h (representative of two experiments). LACC1 and ATG5 levels have been normalized with respect to GAPDH and unstimulated siCTRL condition. The right panels indicate normalized LC3-II (upper), phospho-APMK (middle), and phospho-S6 (lower) to GAPDH. CTRL, control; Norm, normal.

defective de novo lipogenesis via peroxisomal fatty acid synthase interaction (Cader et al., 2016). A very important piece of evidence to support this model was the demonstration, using a commercial anti-LACC1 antibody, that LACC1 localized in peroxisomes. This point was challenged, however, by a subsequent study that used the same commercial antibody (E7 clone; Santa Cruz; Skon-Hegg et al., 2019) and showed a diffuse subcellular localization of LACC1. To test if the discrepancy was due to a lack of specificity of LACC1 antibodies, we stained parental and modified U937 cell lines for LACC1 using antibodies against human influenza hemagglutinin (HA) tag or LACC1, as mentioned above. HA staining, acting as the positive control in this experiment, gave a specific staining in all three applications tested (i.e., WB, flow cytometry, and confocal microscopy; Fig. S1, A and B). In contrast, both Sigma-Aldrich and Santa Cruz antibodies generated nonspecific binding when applied in flow cytometry (Fig. S1 B) and immunofluorescence (Fig. S1 C).

Thus, we explored other mechanisms that may explain the decreased pool of fatty acids in the absence of LACC1. In particular, previous studies established that AMPK-mediated autophagy was essential to promote the generation of lipid droplets (Nguyen et al., 2017). As we identified a physical and functional link between LACC1, AMPK, and autophagy, we tested the impact of LACC1 deficiency on the accumulation of lipid droplets. Red oil staining revealed a dramatic reduction in lipid droplets in LACC1-deficient macrophages compared with controls (Fig. 6 A). Lipid droplets provide fatty acids for mitochondrial respiration via fatty acid oxidation. Extracellular oxygen consumption rate (OCR) analysis in LACC1-deficient macrophages indicated decreased mitochondrial respiration (Fig. 6 B). We next tested whether an extracellular source of fatty acid such as palmitate could restore lipid droplets levels, and hence mitochondrial respiration. Macrophages were preincubated with palmitate for 16 h, and red oil staining showed reconstitution of the lipid droplets pool (Fig. 6 C) and increased mitochondrial respiration (Fig. 6 D).

Moreover, the autophagy machinery has been shown to modulate uptake and clearance of foreign particles or apoptotic bodies (Liao et al., 2012; Martinez et al., 2011; Bonilla et al., 2013). Using either patient-derived or siLACC1-treated macrophages, we showed that LACC1-deficient macrophages had reduced apoptotic bodies uptake and bacterial phagocytosis capacity compared with controls (Fig. S5). These results suggest that LACC1 regulates fundamental macrophage functions such as phagocytosis via the regulation of autophagy.

Discussion

JIA is a heterogeneous inflammatory joint disease of unknown cause, currently classified according to clinical and serological data. Next-generation sequencing has provided a new way to identify genetic causes of the disease in familial forms. In this study, we reported mutations in *LACC1* in four independent JIA families, with fully penetrant chronic rheumatic disease of early onset. Moreover, we show, for the first time, that such mutations impair the expression, and thereby the function, of LACC1. This implies that loss of function of LACC1 contributes to

arthritis pathogenesis. However, the mechanisms underlying this contribution remain poorly understood.

LACC1 was previously associated with lipid metabolism, NOD2 complex, ER stress, and purine nucleotide cycle (Cader et al., 2016, 2020; Lahiri et al., 2017; Huang et al., 2019). However, these pathways are difficult to connect to JIA pathogenesis. Systemic forms of JIA in some LACC1-deficient patients (Wakil et al., 2015) suggested a relation with innate immunity excessive activation. However, we provided various data in this article that do not support a functional link between LACC1 deficiency and these pathways. Lahiri et al. (2017) reported that knockdown of LACC1 in human macrophages was associated with a reduction of at least threefold in TNF and IL-1 β /6/8/10 cytokine production upon TLR and NOD2 stimulation. We were not able to reproduce these results using either gene-edited U937 cells or primary human macrophages. Moreover, we did not observe any aberrant NLRP3 inflammasome-dependent IL-1 β secretion in patient macrophages, whereas Cader et al. (2016) reported a decrease in IL-1 β production in *Lacc1*-knockout murine macrophages following NLRP3 activation. Notably, the same study demonstrated that intraperitoneal injection of LPS resulted in higher IL-1 β secretion in the knockout mouse model, a finding that was not retrieved in a LPS-induced sepsis model (Skon-Hegg et al., 2019). The reasons for these discrepancies remain unclear and warrant further investigation.

In vivo, tissue-resident macrophages have either embryonic or monocytic origin, and are dependent on environment cues for functional specialization. For the first time, we report that M-CSF, and not GM-CSF, strongly induces LACC1 expression during macrophage differentiation via the activation of the mTOR pathway. M-CSF is known to generate anti-inflammatory M2-like macrophages with tissue remodeling functions, while GM-CSF favors the production of inflammatory M1-like macrophages for pathogen elimination (Lacey et al., 2012). It is also possible that similar to Crohn's disease, which has been associated to NOD2 variants, defective phagocytosis in LACC1 patients could participate in systemic inflammation (Travassos et al., 2010). Further studies are required to understand which human macrophage subsets express LACC1 in vivo and the role of microbiota, which may provide insights into the pathophysiology of the disease. One can also speculate that additional genetic or environmental factors may impact LACC1 expression in other juvenile- or adult-onset arthritis.

In our study, mTOR-dependent signals induced LACC1, which promoted autophagy. Both mTOR and autophagy are important in human macrophage differentiation, despite both processes being antagonistic (Zhang et al., 2012; Jacquelin et al., 2009, 2012). M-CSF-activated colony-stimulating factor 1 receptor (CSF1R) triggers cyclic activation of the AKT-mTOR pathway necessary for human macrophage differentiation (Jacquelin et al., 2009). We hypothesize that autophagy follows similar cyclic activation, and that LACC1 might represent a potential switch between these processes. Indeed, loss of LACC1 impaired autophagic flux and increased mTOR signaling in primary macrophages, representing a feed-forward loop to promote LACC1 expression. To counteract the spontaneous mTOR activation and promote autophagy, mTOR inhibition may represent a new avenue for the

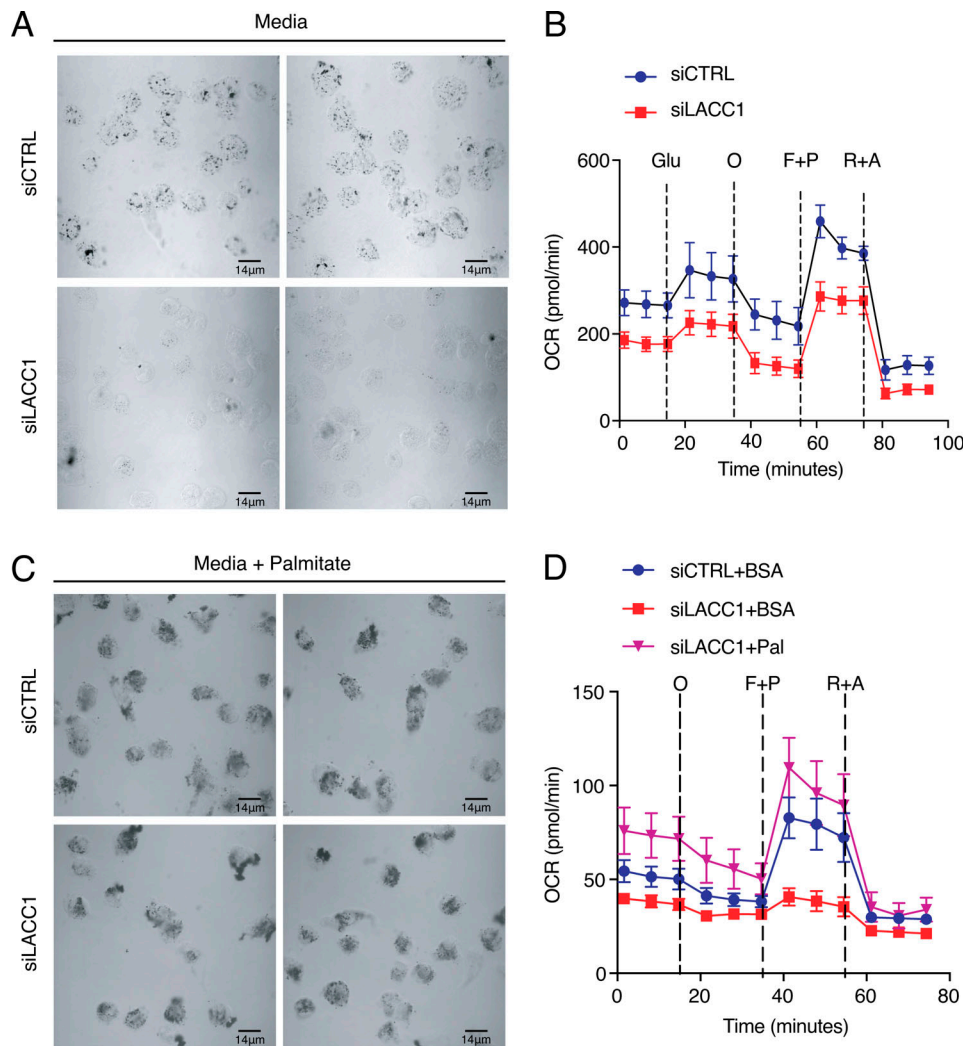


Figure 6. **LACC1 promotes lipid droplet and mitochondrial respiration.** (A) Red oil staining of macrophages transfected with control or LACC1 siRNA in basal RPMI medium (representative of three experiments). (B) OCR measurement of macrophages transfected with control or LACC1 siRNA with successive glucose (Glu), oligomycin (O), FCCP (F+P), and rotenone and antimycin A (R+A) treatments (representative of three experiments). (C) Red oil staining of macrophages transfected with control or LACC1 siRNA in palmitate supplemented medium for 16 h (representative of two experiments). (D) OCR measurement of transfected with control or LACC1 siRNA treated with palmitate followed by successive addition of glucose, oligomycin, FCCP, and rotenone and antimycin A (representative of two experiments). Pal, palmitate.

treatment of inflammatory arthritis (Cejka et al., 2010). In addition, mouse studies have demonstrated the importance of mTOR in fueling glucose and sterol biosynthesis during macrophage differentiation (Karmaus et al., 2017). The present study, and others, indicate that LACC1 (Cader et al., 2016) regulates lipid metabolism. This role may be connected to the shift in lipid metabolism undergone by differentiating macrophages, and suggests a functional impact in vivo (Ecker et al., 2010).

Our study identified RACK1 and AMPK, two autophagy-initiating proteins, as LACC1 partners. LACC1 polymorphisms have been associated with Crohn's disease (Assadi et al., 2016; Cleynen et al., 2013; Huang et al., 2016; Patel et al., 2014; Umeno et al., 2011), and such associations were also observed for variants of several autophagy-associated genes such as NOD2, ATG16L1, and IRGM (Iida et al., 2017). These proteins interact and associate closely with AMPK (Chauhan et al., 2015), while NOD2

partners with LACC1 (Lahiri et al., 2017). These genetic associations consolidate our model that LACC1 binds to the AMPK complex to regulate autophagy. Functionally, we demonstrate a partial reduction of the autophagy flux in LACC1-deficient macrophages under normal culture conditions.

Impaired AMPK activity decreases autophagic flux and limits lipid droplet formation, which can no longer feed mitochondrial respiration (Nguyen et al., 2017). Our study revealed impaired lipid droplet levels and mitochondrial respiration in LACC1-deficient macrophages, which could be compensated by exogenous palmitate. Supplementation of *Lacc1* knockout murine macrophages with fatty acid also rescued mitochondrial respiration (Cader et al., 2016). These results suggest that the composition of the extracellular medium or tissue microenvironment can modulate LACC1-associated phenotypes. One may speculate that the metabolic composition of the joint microenvironment drives a

pro-inflammatory phenotype of LACCI-deficient macrophages. Alternatively, LACCI-dependent autophagy in macrophages may allow the clearance of some joint-specific inflammatory lipids. Indeed, lipid droplets are known to play cytoprotective roles by sequestering fatty acids and reducing the accumulation of various cytotoxic lipid species (Nguyen et al., 2017). Furthermore, based on the known interplay between autophagy and lysosomes, LACCI may also regulate other cellular functions associated with lysosomes such as antigen presentation. Finally, a more global defect of membrane trafficking may also account for the phagocytosis and autophagy defects.

In conclusion, we find that loss-of-function mutations in LACCI are associated with chronic rheumatic disease with full penetrance. Proteomic and biochemical investigations demonstrate a novel role for LACCI in modulating autophagy flux through AMPK signaling. This autophagic flux regulated lipid droplet levels and mitochondrial activity, thus linking LACCI to immunometabolism. LACCI deficiency thus defines a novel category of inflammatory disease associated with macrophage defects in autophagy and metabolism.

Material and methods

Ethics statement

Written informed consent was obtained for data collection, blood sampling, and genetic testing relating to patients, family members, and healthy control subjects. The study was approved by the Leeds (East) Multi-center Research Ethics Committee (no. 10/H1307/132) and the Comité de Protection des Personnes Sud-EST III Ethics Committee (no. 2013-011B).

Exome sequencing

DNA was extracted from whole blood samples using standard methods. Whole-exome sequencing was performed on genomic DNA of patients. Whole-exome sequencing was performed using an AmpliSeq kit, with libraries analyzed on a Life Technologies Proton instrument. P3 was sequenced using a SureSelect Human All Exon kit (Agilent Technologies) for targeted enrichment and an Illumina HiSeq 2000. Variants were assessed using the in silico programs combined annotation-dependent depletion (<https://cadd.gs.washington.edu>), SIFT (<http://sift.jcvi.org>), and Polyphen-2 (<http://genetics.bwh.harvard.edu/pph2/>), and summarized in Varcards (<http://varcards.biols.ac.cn>). Population allele frequencies were obtained from the ExAC (<http://exac.broadinstitute.org>) and Genome Aggregation Database (<http://gnomad.broadinstitute.org>) databases. Sanger sequencing was performed on DNA from patients and their parents to confirm the LACCI variants found by exome sequencing. The reference sequence used for primer design and nucleotide numbering was LACCI (NM_001128303.1). Primer sequences are available on request.

Monocyte purification

Blood was obtained from healthy donors from the Etablissement Français du Sang Auvergne Rhône Alpes, France, under the convention EFS 16-2066. Peripheral blood mononuclear cells were isolated from 450 ml of freshly drawn venous human

peripheral blood by Ficoll (Eurobio) density gradient centrifugation. Cells were washed three times in sterile PBS (Thermo Fisher Scientific) and resuspended in separation medium (PBS, pH 7.2, supplemented with 0.5% BSA and 2 mM EDTA). Monocyte purification was performed by CD14-positive selection using a human CD14 microbeads purification kit (Miltenyi Biotec) following the manufacturer's recommendations. Cell suspensions were always >95% CD14⁺ as determined by flow-cytometric analysis.

Cell line and reagents

Human myeloid cell line U937 was obtained from the biological resource center Cellulonet (Lyon, France) and grown in RPMI 1640 GlutaMax (Thermo Fisher Scientific) supplemented with 10% (vol/vol) heat-inactivated fetal calf serum (Dutscher), 10 mM Hepes, pH 7.5 (Thermo Fisher Scientific), and 0.04 mg/ml gentamycin (Thermo Fisher Scientific). U937 cells were exposed to 100 ng × ml⁻¹ of PMA (InvivoGen) for differentiation. For primary macrophage differentiation, purified monocytes were plated in the presence of 50 ng/ml M-CSF (Miltenyi Biotec) and incubated at 37°C in 5% CO₂ for times indicated in the figure legends. Human GM-CSF and human IL-4 were from Miltenyi Biotec. Rapamycin was from Tocris. Torin 2 and BafA1 were from InvivoGen. The inhibitors SB203580 (p38 inhibitor), SP600125 (JNK inhibitor), PD98059 (ERK inhibitor), and LY294002 (PI3K inhibitor) from InvivoGen and AZD5363 (AKT inhibitor) from Selleckchem were gifts from Patrice André and the Vincent Lotteau Laboratory (Centre International de Recherche en Infectiologie, Lyon, France). Chloroquine, pepstadin A, and E64D were from Sigma-Aldrich, while BafA1 was from InvivoGen. LPS used for macrophages stimulation was from InvivoGen. Heat-killed *S. enterica* serovar Typhimurium (strain SL1344) and heat-killed *S. aureus* (strain Lug960) were cultured in T. Henry's laboratory.

LACCI knockout in U937

LACCI gene expression was invalidated in the U937 cell line by CRISPR/Cas9 technology. Guide RNA (gRNA) directed against LACCI (5'-GCTGTTTTGATTGATCTTTT-3') was cloned into the pSpCas9(BB)-2A-GFP (PX458) vector (from Feng Zhang; Addgene plasmid 48138) following an adapted protocol from the Zhang laboratory (McGovern Institute, Massachusetts Institute of Technology, Cambridge, MA). To generate the knockout cell line, 1 µg of gRNA-expressing plasmid was transfected into 5,104 mycoplasma-free U937 cells using the Neon Transfection System (Thermo Fisher Scientific) according to the manufacturer's protocol (10 µl tips; 1,300 V; 30 ms; one pulse). 2 d later, single-clone GFP-positive cells were sorted by flow cytometry on the BD Biosciences FACSaria II. LACCI knockout clones were screened by sequencing of a PCR fragment corresponding to the genomic region flanking the targeted sequence and by WB.

Introduction of HA tag on endogenous LACCI in U937 cell line

gRNA was designed to target LACCI near ATG using Crispor-Tefor webtool and was synthesized by IDT (gRNA sequence: 5'-TAAAAGTATTCTTTCAAGGA-3'). Single-stranded oligodeoxynucleotide (ssODN) was designed to add HA tag in the

N-terminal part of LACC1 and was synthesized by IDT (5'-GGA CAGCATTCAAAGTCTTCAGTAATGTCTGATGGCAGTTTTTTT GAGAGTTCAATTTCAAACCAAAAAGATCAATCAAAAACAGCTT CTGCGGCATAATCTGGCACATCATAAGGGTACATCCTTGAAA GAATACTTTTATGCCAAATAAATCA-3'). The protocol for delivery of ribonucleoprotein (RNP) and ssODN in U937 was adapted from a protocol available on the IDT website (Alt-R CRISPR/Cas9 system-RNP electroporation Neon transfection system). Briefly, equal volumes of CRISPR RNA (crRNA; 200 μ M in nuclease-free duplex buffer; IDT) and transactivating crRNA (tracrRNA; 200 μ M in nuclease-free duplex buffer; IDT) were mixed, heated at 95°C for 5 min, cooled slowly at room temperature for 30 min, and then plunged into ice to form the single-guide RNA (sgRNA). sgRNA was then diluted to 43 μ M in nuclease-free duplex buffer (IDT). Cas9 (Alt-R S.p. Cas9 Nuclease V3; IDT) was diluted to 36 μ M in buffer R from the Neon transfection system kit (10 μ l; Thermo Fisher Scientific). For one reaction, 0.5 μ l of sgRNA was mixed with 0.5 μ l of diluted Cas9, and the mixture (RNP mix) was incubated 20 min at room temperature. 5×10^5 U937 cells were centrifuged and washed once in PBS, then resuspended in 9 μ l R buffer from the Neon transfection system kit (10 μ l; Thermo Fisher Scientific). 1 μ l of RNP mix was added to the cell suspension with 2 μ l of 10.8 μ M solution of Alt-R Cas9 Electroporation Enhancer (IDT) and 1 μ l of ssODN (30 μ M stock in IDT nuclease-free duplex buffer). Cells were electroporated using the Neon system (Thermo Fisher Scientific; 1,300 V; 30 ms; one pulse).

10 μ l electroporated cells were added to 190 μ l complete pre-warmed medium and grown for several days. 4 d after electroporation, genomic DNA flanking the region of interest was sequenced to confirm the presence of genome editing. Then U937 was cloned, and clones were screened by PCR to confirm the presence of endogenous LACC1 HA tag (by PCR and WB).

siRNA transfection in macrophages

After 4 d of macrophage differentiation, medium was removed and replaced by 8 ml of fresh RPMI containing M-CSF. siRNA (Dharmacon) complexes were prepared at a concentration of 10 nM and were transfected using Lipofectamine RNAiMAX reagent (Thermo Fisher Scientific) according to the manufacturer's instructions. ON-TARGETplus Non-targeting Pool (D-001810-10) was used as a negative control. ON-TARGETplus LACC1 (L-015653-02) and ATG5 (L-004374-00) siRNA were used to decrease LACC1 and ATG5 protein expression, respectively.

IFN score assessment

Total RNA extraction was performed on whole blood collected on EDTA using a Maxwell 16 LEV SimplyRNA Blood Kit (Promega) and a magnetic particle processor (Maxwell 16; Promega) according to the manufacturer's recommendations. The extraction kit included an individual DNase treatment. Total RNA was diluted in 40 μ l RNase free water, and the concentration was quantified by spectrophotometry using a NanoVue (Biochrom). The IFN signature was assessed using the NanoString (NanoString Technologies) procedure; 200 ng of RNA was hybridized to the probes (a reporter probe and a

capture probe) at 67°C for 16–21 h using a thermocycler. Samples were then inserted into the nCounter Prep Station for the removal of excessive probes, purification, and immobilization onto the internal surface of a sample cartridge for 2–3 h. Finally, the sample cartridge was transferred to the nCounter Digital Analyzer, where color codes were counted and tabulated for each target molecule. Count numbers obtained for the six ISGs were normalized by the geometric mean of three housekeeping genes count numbers (β -actin, HPRT1 [hypoxanthine phosphoribosyltransferase 1] and POLR2A [RNA polymerase II subunit A]) as well as the negative and positive control values using nSolver software.

HeLa cell transfection

HeLa cells stably expressing LC3-GFP were cultured in DMEM with Glutamax supplemented with 10% fetal bovine serum, 10 mM HEPES, and 40 μ g/ml gentamycin (Thermo Fisher Scientific). Cells were seeded at 150,000 cells per well in 6-well culture dishes for transfection. Cells were transfected with p3XFlag-CMV-hsLACC1 vector coding for human LACC1 cDNA fused to 3xFlag tag in its N-terminal sequence using the jetPEI reagent (Polyplus Transfection) according to the manufacturer's instructions.

Immunofluorescence

1.5×10^5 HeLa and 3×10^5 U937 cells were seeded on glass coverslips in 24-well plates and stimulated the next day as indicated. At the desired time points, cells were washed three times with PBS and were fixed for 10 min with 4% paraformaldehyde. Following fixation, coverslips were washed three times with PBS and incubated 5 min with 0.1% Triton X-100. Coverslips were washed three times with PBS, and after 20 min incubation with blocking buffer (PBS, 10% goat serum, 3% BSA, and 1% human serum), coverslips were stained overnight at 4°C with mouse and rabbit primary antibodies for 20 min at room temperature with the following secondary antibodies: goat anti-mouse-Alexa Fluor 488 (Sigma-Aldrich; 1:1,000), and goat anti-rabbit-Alexa Fluor 647 (Sigma-Aldrich; 1:1,000). Following a 10-min staining with DAPI (Vector Labs), coverslips were mounted on glass slides with Prolong Gold (Molecular Probes) and imaged on a Zeiss LSM710.

Inflammasome activation assay

Macrophages were seeded in 96-well plates at 5×10^4 cells/well in RPMI 1640 GlutaMAX medium (Thermo Fisher Scientific) supplemented with 10% fetal calf serum (Dutscher). Macrophages were incubated for 3 h in the presence or absence of a priming signal consisting of LPS (10 ng/ml; Invivogen). Cells were then treated for 1.5 h with nigericin (5 mM; Invivogen) for NLRP3 inflammasome activation. Following the incubation, cells were centrifuged, and supernatants were collected.

Cytokine release measurement

All ELISAs were from R&D Systems (DY210 and DY201) and were used following the manufacturer's recommendations. Briefly, 50,000 macrophages were stimulated with 10 ng/ml of LPS for 3 h followed by 5 μ M with nigericin for 1 h 30 min. Supernatants were collected and assayed for IL-1 β and TNF levels.

Immunoblot analysis

Cells were lysed in NP-40 lysis buffer (20 mM Tris, HCl, pH 7.4, 150 mM NaCl, 2 mM EDTA, and 1% NP-40) containing protease inhibitors for 30 min at 4°C. Supernatant was collected following 10 min centrifugation at 16,000 g, 4°C, and protein content was quantified using the μ BCA quantification kit (Thermo Fisher Scientific). Protein extracts (50 μ g) were separated by SDS-PAGE on precast 4–12% acrylamide gel gradients and transferred to TransBlot Turbo Midi-size nitrocellulose membranes (Bio-Rad). Antibodies used were anti-LACC1 (E7 clone; Santa Cruz), anti-GAPDH, anti-IL-1 β , anti-phospho and total Akt, AMPK, IK β , IKK β , and S6 from Cell Signaling Technology, anti-LC3B from Sigma-Aldrich, anti-p62 from Abcam, and anti-rabbit IgG antibody conjugated to horseradish peroxidase (1:10,000; Jackson ImmunoResearch), and revealed using the Chemiluminescence Western Lightening Plus Kit (Perkin-Elmer).

Flow cytometry analysis

U937 cells were fixed with eBioscience Fixation/Permeabilization Concentrate (00-5123-43; Invivogen) in combination with the 10 \times Permeabilization buffer (00-8333-56) following the manufacturer's instructions. Cells were then stained with primary antibodies (anti-LACC1 [E7 clone; Santa Cruz], anti-LACC1 [HPA040150; Sigma-Aldrich], or anti-HA [901524; Biolegend]) for 1 h at room temperature. Secondary antibodies used were anti-rabbit or anti-mouse coupled with Alexa Fluor 747 for 30 min. Cells were then acquired using a LSRFortessa (BD Biosciences), and data were analyzed using FlowJo (version 10.2)

Bimolecular fluorescence complementation (BiFC) screen

HEK293T cells were established with a library of 7474 human ORFs fused to the C-terminal fragment of Cerulean (CC) and under the control of a Dox-inducible promoter. The library was inserted at one copy/cell for the large majority (80%) of cells. A proof-of-principle of this tool has been deposited (patent FR1655539), and more information will be described elsewhere (unpublished data). Transfections of the BiFC-human embryonic kidney (HEK) 293T cell library with the VN-LACC1 encoding plasmid were performed using the JetPRIME reagent (Polyplus).

Red oil staining

300,000 cells were plated onto coverslips in 24-well plates and allowed to rest overnight before being stimulated the next day as indicated. Cells were washed with PBS and fixed for 20 min with 4% paraformaldehyde and permeabilized with 70% isopropanol for 5 min. Cell were then stained with a solution of 4.2 mM Red Oil O dissolved in isopropanol for 15 min followed by several washes with water. Coverslips were then mounted onto glass slides using ProLong Gold Antifade Mountant (P36934; Thermo Fisher Scientific). Slides were analyzed on an LSM 800 confocal microscope, and ImageJ was used to process the images.

Seahorse analysis

The OCR was measured in XF medium (unbuffered RPMI containing 2 mM glutamine, pH 7.4) under basal conditions and in response to glucose (25 mM), oligomycin (1 μ M), trifluoromethoxy carbonylcyanide phenylhydrazide (FCCP; 1.5 M), plus pyruvate

(1 mM) and antimycin A (1 μ M), plus rotenone (0.1 μ M) with an XFp Extracellular Flux Analyzer (Seahorse Bioscience). Macrophages were plated (2×10^5 cells per well) in Seahorse plates overnight. The OCR was analyzed in real time for 155 min. For the fatty acid supplementation assay, Seahorse XF Palmitate-BSA FAO Substrate kit (Agilent) was used according to the manufacturer's instructions.

Efferocytosis assay

Murine thymocytes were stained using 1 μ M of CFSE (Life Technologies) for 10 min at 37°C and washed two times with 30 ml of complemented RPMI medium. Cells were treated for 4 h with dexamethasone (Sigma-Aldrich) to induce apoptosis. The CFSE-stained apoptotic bodies were washed twice with supplemented RPMI medium before being used in the efferocytosis assay. 1×10^4 macrophages were seeded on a 48-well plate overnight. 1×10^5 CFSE-stained apoptotic thymocytes were added to macrophages for 2 h. Macrophages were washed with PBS, trypsinized, and resuspended in 200 μ l of PBS. CFSE uptake was analyzed by flow cytometry.

Phagocytosis assay

Briefly, 5×10^4 macrophages seeded on a 24-well plate overnight and were incubated with DsRed-expressing *Escherichia coli* at a multiplicity of infection of 10 in antibiotic-free RPMI medium for 30 min. Wells were then washed twice with PBS, and gentamycin-containing RPMI was added. Macrophages were incubated for indicated times. Macrophages were washed with PBS, trypsinized, and resuspended in 200 μ l of PBS before analysis by flow cytometry.

Statistical analysis

Data were analyzed in GraphPad Prism 5.0. Appropriate use of unpaired and paired *t* tests was made to calculate significant differences between different experimental conditions. These are mentioned in the figure legends.

Online supplemental material

Fig. S1 shows the specificity of various anti-LACC1 antibodies for different protein detection assays. Fig. S2 shows the implication of signaling pathways modulating LACC1 expression. Fig. S3 shows the inflammatory profile in LACC1-deficient patients. Fig. S4 shows the implication of LACC1 in the autophagy machinery using primary human macrophages or a reporter HeLa LC3-GFP cell line. Fig. S5 shows the phagocytic capacity of LACC1-deficient macrophages in response to apoptotic bodies or bacteria.

Acknowledgments

We thank Sae Lim von Stuckrad for organizing the transport of clinical samples of Family A.

This work was supported by grants from Societe Francaise de Rhumatologie (grant 2016) and Fondation pour la Recherche Medicale (FDT201805005237).

Author contributions: O. Omarjee designed, performed, and analyzed experiments. A.-L. Mathieu performed and analyzed

experiments. G. Quiniou and M. Faure conceptualized the autophagy experiments. M. Moreews performed experiments. M. Ainouze performed experiments. C. Frachette, M. Gerfaud-Valentin, A. Duquesne, Y. Jamilloux, and J.-P. Larbre provided clinical samples and data of Family C. I. Melki, C. Dumaine, and G. Sarrabay provided clinical samples and data of Family D. S. Georgin-Lavialle provided clinical samples and data of Family B. T. Kallinich provided clinical samples and data of Family A. E. Tahir Turanli provided clinical samples. C. Malcus performed immunophenotyping of patients. S. Viel and R. Pescarmona performed IFN signatures of patients. G.I. Rice and Y. J. Crow provided genetic analysis of Family C. F. Magnotti and T. Henry conceptualized the inflammasome assays. F. Bleicher, J. Reboulet, and S. Merabet designed and performed the proteomic screen. T. Walzer and A. Belot supervised, designed, and funded this study. O. Omarjee prepared the initial draft. T. Walzer and A. Belot reviewed and finalized the paper.

Disclosures: S. Georgin-Lavialle reported personal fees from SOBI, non-financial support from Novartis, and personal fees from BMS outside the submitted work. F. Bleicher reported a patent to FR1655539 pending. J. Reboulet reported a patent to FR1655539 issued. S. Merabet reported a patent to FR1655539 pending. T. Henry reported personal fees from SOBI and grants from SOBI outside the submitted work. No other disclosures were reported.

Submitted: 17 May 2020

Revised: 16 September 2020

Accepted: 22 December 2020

References

- Aksentijevich, I., and Q. Zhou. 2017. NF- κ B Pathway in Autoinflammatory Diseases: Dysregulation of Protein Modifications by Ubiquitin Defines a New Category of Autoinflammatory Diseases. *Front. Immunol.* 8:399. <https://doi.org/10.3389/fimmu.2017.00399>
- Assadi, G., R. Saleh, F. Hadizadeh, L. Vesterlund, F. Bonfiglio, J. Halfvarson, L. Törkvist, A.S. Eriksson, H.E. Harris, E. Sundberg, and M. D'Amato. 2016. LACC1 polymorphisms in inflammatory bowel disease and juvenile idiopathic arthritis. *Genes Immun.* 17:261–264. <https://doi.org/10.1038/gene.2016.17>
- Baldassano, R.N., J.P. Bradfield, D.S. Monos, C.E. Kim, J.T. Glessner, T. Casalanovo, E.C. Frackelton, F.G. Otieno, S. Kanterakis, J.L. Shaner, et al. 2007. Association of the T300A non-synonymous variant of the ATG16L1 gene with susceptibility to paediatric Crohn's disease. *Gut.* 56: 1171–1173. <https://doi.org/10.1136/gut.2007.122747>
- Bonilla, D.L., A. Bhattacharya, Y. Sha, Y. Xu, Q. Xiang, A. Kan, C. Jagannath, M. Komatsu, and N.T. Eissa. 2013. Autophagy regulates phagocytosis by modulating the expression of scavenger receptors. *Immunity.* 39: 537–547. <https://doi.org/10.1016/j.immuni.2013.08.026>
- Cader, M.Z., K. Boroviak, Q. Zhang, G. Assadi, S.L. Kempster, G.W. Sewell, S. Saveljeva, J.W. Ashcroft, S. Clare, S. Mukhopadhyay, et al. 2016. C13orf31 (FAMIN) is a central regulator of immunometabolic function. *Nat. Immunol.* 17:1046–1056. <https://doi.org/10.1038/ni.3532>
- Cader, M.Z., R.P. de Almeida Rodrigues, J.A. West, G.W. Sewell, M.N. Mdlbrahim, S. Reikine, G. Sirago, L.W. Unger, A.B. Iglesias-Romero, K. Ramshorn, et al. 2020. FAMIN Is a Multifunctional Purine Enzyme Enabling the Purine Nucleotide Cycle. *Cell.* 180:278–295.e23. <https://doi.org/10.1016/j.cell.2019.12.017>
- Carta, S., F. Penco, R. Lavieri, A. Martini, C.A. Dinarello, M. Gattorno, and A. Rubartelli. 2015. Cell stress increases ATP release in NLRP3 inflammasome-mediated autoinflammatory diseases, resulting in cytokine imbalance. *Proc. Natl. Acad. Sci. USA.* 112:2835–2840. <https://doi.org/10.1073/pnas.1424741112>
- Cejka, D., S. Hayer, B. Niederreiter, W. Sieghart, T. Fuereder, J. Zwerina, and G. Schett. 2010. Mammalian target of rapamycin signaling is crucial for joint destruction in experimental arthritis and is activated in osteoclasts from patients with rheumatoid arthritis. *Arthritis Rheum.* 62:2294–2302. <https://doi.org/10.1002/art.27504>
- Chauhan, S., M.A. Mandell, and V. Deretic. 2015. IRGM governs the core autophagy machinery to conduct antimicrobial defense. *Mol. Cell.* 58: 507–521. <https://doi.org/10.1016/j.molcel.2015.03.020>
- Cleyen, I., J.R. González, C. Figueroa, A. Franke, D. McGovern, M. Bortlik, B.J.A. Crusius, M. Vecchi, M. Artieda, M. Szczypiorska, et al. 2013. Genetic factors conferring an increased susceptibility to develop Crohn's disease also influence disease phenotype: results from the IBDchip European Project. *Gut.* 62:1556–1565. <https://doi.org/10.1136/gutjnl-2011-300777>
- Dennis, G. Jr., C.T.J. Holweg, S.K. Kummerfeld, D.F. Choy, A.F. Setiadi, J.A. Hackney, P.M. Haverty, H. Gilbert, W.Y. Lin, L. Diehl, et al. 2014. Synovial phenotypes in rheumatoid arthritis correlate with response to biologic therapeutics. *Arthritis Res. Ther.* 16:R90. <https://doi.org/10.1186/ar4555>
- Ecker, J., G. Liebisch, M. Englmaier, M. Grandl, H. Robenek, and G. Schmitz. 2010. Induction of fatty acid synthesis is a key requirement for phagocytic differentiation of human monocytes. *Proc. Natl. Acad. Sci. USA.* 107:7817–7822. <https://doi.org/10.1073/pnas.0912059107>
- Erbil, S., O. Oral, G. Mitou, C. Kig, E. Durmaz-Timucin, E. Guven-Maiorov, F. Gulacti, G. Gokce, J. Dengjel, O.U. Sezerman, and D. Gozuacik. 2016. RACK1 Is an Interaction Partner of ATG5 and a Novel Regulator of Autophagy. *J. Biol. Chem.* 291:16753–16765. <https://doi.org/10.1074/jbc.M115.708081>
- Evans, H.G., N.J. Gullick, S. Kelly, C. Pitzalis, G.M. Lord, B.W. Kirkham, and L.S. Taams. 2009. In vivo activated monocytes from the site of inflammation in humans specifically promote Th17 responses. *Proc. Natl. Acad. Sci. USA.* 106:6232–6237. <https://doi.org/10.1073/pnas.0808144106>
- Firestein, G.S., and I.B. McInnes. 2017. Immunopathogenesis of Rheumatoid Arthritis. *Immunity.* 46:183–196. <https://doi.org/10.1016/j.immuni.2017.02.006>
- Grinberg, A.V., C.-D. Hu, and T.K. Kerppola. 2004. Visualization of Myc/Mad family dimers and the competition for dimerization in living cells. *Mol. Cell. Biol.* 24:4294–4308. <https://doi.org/10.1128/MCB.24.10.4294-4308.2004>
- Harapas, C.R., A. Steiner, S. Davidson, and S.L. Masters. 2018. An Update on Autoinflammatory Diseases: Inflammationopathies. *Curr. Rheumatol. Rep.* 20:40. <https://doi.org/10.1007/s11926-018-0750-4>
- Harris, J., M. Hartman, C. Roche, S.G. Zeng, A. O'Shea, F.A. Sharp, E.M. Lambe, E.M. Creagh, D.T. Golenbock, J. Tschopp, et al. 2011. Autophagy controls IL-1 β secretion by targeting pro-IL-1 β for degradation. *J. Biol. Chem.* 286:9587–9597. <https://doi.org/10.1074/jbc.M110.202911>
- Hersh, A.O., and S. Prahalad. 2015. Immunogenetics of juvenile idiopathic arthritis: A comprehensive review. *J. Autoimmun.* 64:113–124. <https://doi.org/10.1016/j.jaut.2015.08.002>
- Homer, C.R., A.L. Richmond, N.A. Rebert, J.P. Achkar, and C. McDonald. 2010. ATG16L1 and NOD2 interact in an autophagy-dependent antibacterial pathway implicated in Crohn's disease pathogenesis. *Gastroenterology.* 139:1630–1641, 1641.e1–2. <https://doi.org/10.1053/j.gastro.2010.07.006>
- Huang, C., S.S. De Ravin, A.R. Paul, T. Heller, N. Ho, L. Wu Datta, C.S. Zerbe, B.E. Marciano, D.B. Kuhns, H.A. Kader, et al. NIDDK IBD Genetics Consortium. 2016. Genetic Risk for Inflammatory Bowel Disease Is a Determinant of Crohn's Disease Development in Chronic Granulomatous Disease. *Inflamm. Bowel Dis.* 22:2794–2801. <https://doi.org/10.1097/MIB.0000000000000966>
- Huang, C., M. Hedl, K. Ranjan, and C. Abraham. 2019. LACC1 Required for NOD2-Induced, ER Stress-Mediated Innate Immune Outcomes in Human Macrophages and LACC1 Risk Variants Modulate These Outcomes. *Cell Rep.* 29:4525–4539.e4. <https://doi.org/10.1016/j.celrep.2019.11.105>
- Iida, T., K. Onodera, and H. Nakase. 2017. Role of autophagy in the pathogenesis of inflammatory bowel disease. *World J. Gastroenterol.* 23: 1944–1953. <https://doi.org/10.3748/wjg.v23.i11.1944>
- Jacquel, A., N. Benikhlef, J. Paggetti, N. Lalaoui, L. Guery, E.K. Dufour, M. Ciudad, C. Racœur, O. Micheau, L. Delva, et al. 2009. Colony-stimulating factor-1-induced oscillations in phosphatidylinositol-3 kinase/AKT are required for caspase activation in monocytes undergoing differentiation into macrophages. *Blood.* 114:3633–3641. <https://doi.org/10.1182/blood-2009-03-208843>

- Jacquel, A., S. Obba, L. Boyer, M. Dufies, G. Robert, P. Gounon, E. Lemichez, F. Luciano, E. Solary, and P. Auberger. 2012. Autophagy is required for CSF-1-induced macrophagic differentiation and acquisition of phagocytic functions. *Blood*. 119:4527–4531. <https://doi.org/10.1182/blood-2011-11-392167>
- Kallinich, T., A. Thorwarth, S.-L. von Stuckrad, A. Rösen-Wolff, H. Luksch, P. Hundsdoerfer, K. Minden, and P. Krawitz. 2016. Juvenile arthritis caused by a novel FAMIN1 (LACC1) mutation in two children with systemic and extended oligoarticular course. *Pediatr. Rheumatol. Online J.* 14:63. <https://doi.org/10.1186/s12969-016-0124-2>
- Kannan, M., E. Bayam, C. Wagner, B. Rinaldi, P.F. Kretz, P. Tilly, M. Roos, L. McGillevie, S. Bär, S. Minocha, et al. Sanger Mouse Genetics Project. 2017. WD40-repeat 47, a microtubule-associated protein, is essential for brain development and autophagy. *Proc. Natl. Acad. Sci. USA*. 114: E9308–E9317. <https://doi.org/10.1073/pnas.1713625114>
- Karacan, I., S. Uğurlu, S. Şahin, E. Everest, Ö. Kasapçopur, A. Tolun, H. Özdoğan, and E.T. Turanlı. 2018. LACC1 Gene Defects in Familial Form of Juvenile Arthritis. *J. Rheumatol.* 45:726–728. <https://doi.org/10.3899/jrheum.170834>
- Karmaus, P.W.F., A.A. Herrada, C. Guy, G. Neale, Y. Dhungana, L. Long, P. Vogel, J. Avila, C.B. Clish, and H. Chi. 2017. Critical roles of mTORC1 signaling and metabolic reprogramming for M-CSF-mediated myelopoiesis. *J. Exp. Med.* 214:2629–2647. <https://doi.org/10.1084/jem.20161855>
- Klionsky, D.J., H. Abeliovich, P. Agostinis, D.K. Agrawal, G. Aliev, D.S. Askew, M. Baba, E.H. Baehrecke, B.A. Bahr, A. Ballabio, et al. 2008. Guidelines for the use and interpretation of assays for monitoring autophagy in higher eukaryotes. *Autophagy*. 4:151–175. <https://doi.org/10.4161/auto.5338>
- Lacey, D.C., A. Achuthan, A.J. Fleetwood, H. Dinh, J. Roiniotis, G.M. Scholz, M.W. Chang, S.K. Beckman, A.D. Cook, and J.A. Hamilton. 2012. Defining GM-CSF- and macrophage-CSF-dependent macrophage responses by in vitro models. *J. Immunol.* 188:5752–5765. <https://doi.org/10.4049/jimmunol.1103426>
- Lahiri, A., M. Hedl, J. Yan, and C. Abraham. 2017. Human LACC1 increases innate receptor-induced responses and a LACC1 disease-risk variant modulates these outcomes. *Nat. Commun.* 8:15614. <https://doi.org/10.1038/ncomms15614>
- Levine, B., and G. Kroemer. 2019. Biological Functions of Autophagy Genes: A Disease Perspective. *Cell*. 176:11–42. <https://doi.org/10.1016/j.cell.2018.09.048>
- Liao, X., J.C. Sluimer, Y. Wang, M. Subramanian, K. Brown, J.S. Pattison, J. Robbins, J. Martinez, and I. Tabas. 2012. Macrophage autophagy plays a protective role in advanced atherosclerosis. *Cell Metab.* 15:545–553. <https://doi.org/10.1016/j.cmet.2012.01.002>
- Manthiram, K., Q. Zhou, I. Aksentjevich, and D.L. Kastner. 2017. The monogenic autoinflammatory diseases define new pathways in human innate immunity and inflammation. *Nat. Immunol.* 18:832–842. <https://doi.org/10.1038/ni.3777>
- Martinez, J., J. Almendinger, A. Oberst, R. Ness, C.P. Dillon, P. Fitzgerald, M.O. Hengartner, and D.R. Green. 2011. Microtubule-associated protein 1 light chain 3 alpha (LC3)-associated phagocytosis is required for the efficient clearance of dead cells. *Proc. Natl. Acad. Sci. USA*. 108: 17396–17401. <https://doi.org/10.1073/pnas.1113421108>
- Miao, Y., Q. Lv, S. Qiao, L. Yang, Y. Tao, W. Yan, P. Wang, N. Cao, Y. Dai, and Z. Wei. 2019. Alpinetin improves intestinal barrier homeostasis via regulating AhR/suv39h1/TSC2/mTORC1/autophagy pathway. *Toxicol. Appl. Pharmacol.* 384:114772. <https://doi.org/10.1016/j.taap.2019.114772>
- Mizushima, N., T. Yoshimori, and B. Levine. 2010. Methods in mammalian autophagy research. *Cell*. 140:313–326. <https://doi.org/10.1016/j.cell.2010.01.028>
- Nguyen, T.B., S.M. Louie, J.R. Daniele, Q. Tran, A. Dillin, R. Zoncu, D.K. Nomura, and J.A. Olzmann. 2017. DGAT1-Dependent Lipid Droplet Biogenesis Protects Mitochondrial Function during Starvation-Induced Autophagy. *Dev. Cell*. 42:9–21.e5. <https://doi.org/10.1016/j.devcel.2017.06.003>
- Patel, N., M.I. El Mouzan, S.M. Al-Mayouf, N. Adly, J.Y. Mohamed, M.A. Al Mofarreh, N. Ibrahim, Y. Xiong, Q. Zhao, K.A. Al-Saleem, and F.S. Alkuraya. 2014. Study of Mendelian forms of Crohn's disease in Saudi Arabia reveals novel risk loci and alleles. *Gut*. 63:1831–1832. <https://doi.org/10.1136/gutjnl-2014-307859>
- Pescarmona, R., A. Belot, M. Villard, L. Besson, J. Lopez, I. Mosnier, A.-L. Mathieu, C. Lombard, L. Garnier, C. Frachette, et al. 2019. Comparison of RT-qPCR and Nanostring in the measurement of blood interferon response for the diagnosis of type I interferonopathies. *Cytokine*. 113: 446–452. <https://doi.org/10.1016/j.cyto.2018.10.023>
- Philpott, D.J., M.T. Sorbara, S.J. Robertson, K. Croitoru, and S.E. Girardin. 2014. NOD proteins: regulators of inflammation in health and disease. *Nat. Rev. Immunol.* 14:9–23. <https://doi.org/10.1038/nri3565>
- Prakken, B., S. Albani, and A. Martini. 2011. Juvenile idiopathic arthritis. *Lancet*. 377:2138–2149. [https://doi.org/10.1016/S0140-6736\(11\)60244-4](https://doi.org/10.1016/S0140-6736(11)60244-4)
- Rabionet, R., A. Remesal, A. Mensa-Vilaró, S. Murías, R. Alcobendas, E. González-Roca, E. Ruiz-Ortiz, J. Antón, E. Iglesias, C. Modesto, et al. 2019. Biallelic loss-of-function LACC1/FAMIN Mutations Presenting as Rheumatoid Factor-Negative Polyarticular Juvenile Idiopathic Arthritis. *Sci. Rep.* 9:4579. <https://doi.org/10.1038/s41598-019-40874-2>
- Rice, G.I., G.M. Forte, M. Szykiewicz, D.S. Chase, A. Aeby, M.S. Abdel-Hamid, S. Ackroyd, R. Allcock, K.M. Bailey, U. Balottin, et al. 2013. Assessment of interferon-related biomarkers in Aicardi-Goutières syndrome associated with mutations in TREX1, RNASEH2A, RNASEH2B, RNASEH2C, SAMHD1, and ADAR: a case-control study. *Lancet Neurol.* 12:1159–1169. [https://doi.org/10.1016/S1474-4422\(13\)70258-8](https://doi.org/10.1016/S1474-4422(13)70258-8)
- Rodero, M.P., and Y.J. Crow. 2016. Type I interferon-mediated monogenic autoinflammation: The type I interferonopathies, a conceptual overview. *J. Exp. Med.* 213:2527–2538. <https://doi.org/10.1084/jem.20161596>
- Saitoh, T., N. Fujita, M.H. Jang, S. Uematsu, B.-G. Yang, T. Satoh, H. Omori, T. Noda, N. Yamamoto, M. Komatsu, et al. 2008. Loss of the autophagy protein Atg16L1 enhances endotoxin-induced IL-1beta production. *Nature*. 456:264–268. <https://doi.org/10.1038/nature07383>
- Sales-Marques, C., H. Salomão, V.M. Fava, L.E. Alvarado-Arnez, E.P. Amaral, C.C. Cardoso, I.M.F. Dias-Batista, W.L. da Silva, P. Medeiros, M. da Cunha Lopes Virmond, et al. 2014. NOD2 and CCDC122-LACC1 genes are associated with leprosy susceptibility in Brazilians. *Hum. Genet.* 133: 1525–1532. <https://doi.org/10.1007/s00439-014-1502-9>
- Schmelzle, T., T. Beck, D.E. Martin, and M.N. Hall. 2004. Activation of the RAS/cyclic AMP pathway suppresses a TOR deficiency in yeast. *Mol. Cell Biol.* 24:338–351. <https://doi.org/10.1128/MCB.24.1.338-351.2004>
- Singh, R., S. Kaushik, Y. Wang, Y. Xiang, I. Novak, M. Komatsu, K. Tanaka, A.M. Cuervo, and M.J. Czaja. 2009. Autophagy regulates lipid metabolism. *Nature*. 458:1131–1135. <https://doi.org/10.1038/nature07976>
- Skon-Hegg, C., J. Zhang, X. Wu, M. Sagolla, N. Ota, A. Wuster, J. Tom, E. Doran, N. Ramamoorthi, P. Caplazi, et al. 2019. LACC1 Regulates TNF and IL-17 in Mouse Models of Arthritis and Inflammation. *J. Immunol.* 202:183–193. <https://doi.org/10.4049/jimmunol.1800636>
- Spengler, K., N. Kryeziu, S. Große, A.S. Mosig, and R. Heller. 2020. VEGF Triggers Transient Induction of Autophagy in Endothelial Cells via AMPK α 1. *Cells*. 9:687. <https://doi.org/10.3390/cells9030687>
- Steiner, A., C.R. Harapas, S.L. Masters, and S. Davidson. 2018. An Update on Autoinflammatory Diseases: Relopathies. *Curr. Rheumatol. Rep.* 20:39. <https://doi.org/10.1007/s11926-018-0749-x>
- Tassi, S., S. Carta, L. Delfino, R. Caorsi, A. Martini, M. Gattorno, and A. Rubartelli. 2010. Altered redox state of monocytes from cryopyrin-associated periodic syndromes causes accelerated IL-1beta secretion. *Proc. Natl. Acad. Sci. USA*. 107:9789–9794. <https://doi.org/10.1073/pnas.1000779107>
- Travassos, L.H., L.A.M. Carneiro, M. Ramjeet, S. Hussey, Y.-G. Kim, J.G. Magalhães, L. Yuan, F. Soares, E. Chea, L. Le Bourhis, et al. 2010. Nod1 and Nod2 direct autophagy by recruiting ATG16L1 to the plasma membrane at the site of bacterial entry. *Nat. Immunol.* 11:55–62. <https://doi.org/10.1038/ni.1823>
- Umeno, J., K. Asano, T. Matsushita, T. Matsumoto, Y. Kiyohara, M. Iida, Y. Nakamura, N. Kamatani, and M. Kubo. 2011. Meta-analysis of published studies identified eight additional common susceptibility loci for Crohn's disease and ulcerative colitis. *Inflamm. Bowel Dis.* 17:2407–2415. <https://doi.org/10.1002/ibd.21651>
- Wakil, S.M., D.M. Monies, M. Abouelhoda, N. Al-Tassan, H. Al-Dusery, E.A. Naim, B. Al-Younes, J. Shinwari, F.A. Al-Mohanna, B.F. Meyer, and S. Al-Mayouf. 2015. Association of a mutation in LACC1 with a monogenic form of systemic juvenile idiopathic arthritis. *Arthritis Rheumatol.* 67: 288–295. <https://doi.org/10.1002/art.38877>
- Wildenberg, M.E., A.C.W. Vos, S.C.S. Wolfkamp, M. Duijvestein, A.P. Verhaar, A.A. Te Velde, G.R. van den Brink, and D.W. Hommes. 2012. Autophagy attenuates the adaptive immune response by destabilizing the immunologic synapse. *Gastroenterology*. 142:1493–503.e6. <https://doi.org/10.1053/j.gastro.2012.02.034>
- Zhang, Y., M.J. Morgan, K. Chen, S. Choksi, and Z.G. Liu. 2012. Induction of autophagy is essential for monocyte-macrophage differentiation. *Blood*. 119:2895–2905. <https://doi.org/10.1182/blood-2011-08-372383>
- Zhao, Y., Q. Wang, G. Qiu, S. Zhou, Z. Jing, J. Wang, W. Wang, J. Cao, K. Han, Q. Cheng, et al. 2015. RACK1 Promotes Autophagy by Enhancing the Atg14L-Beclin 1-Vps34-Vps15 Complex Formation upon Phosphorylation by AMPK. *Cell Rep.* 13:1407–1417. <https://doi.org/10.1016/j.celrep.2015.10.011>

Supplemental material

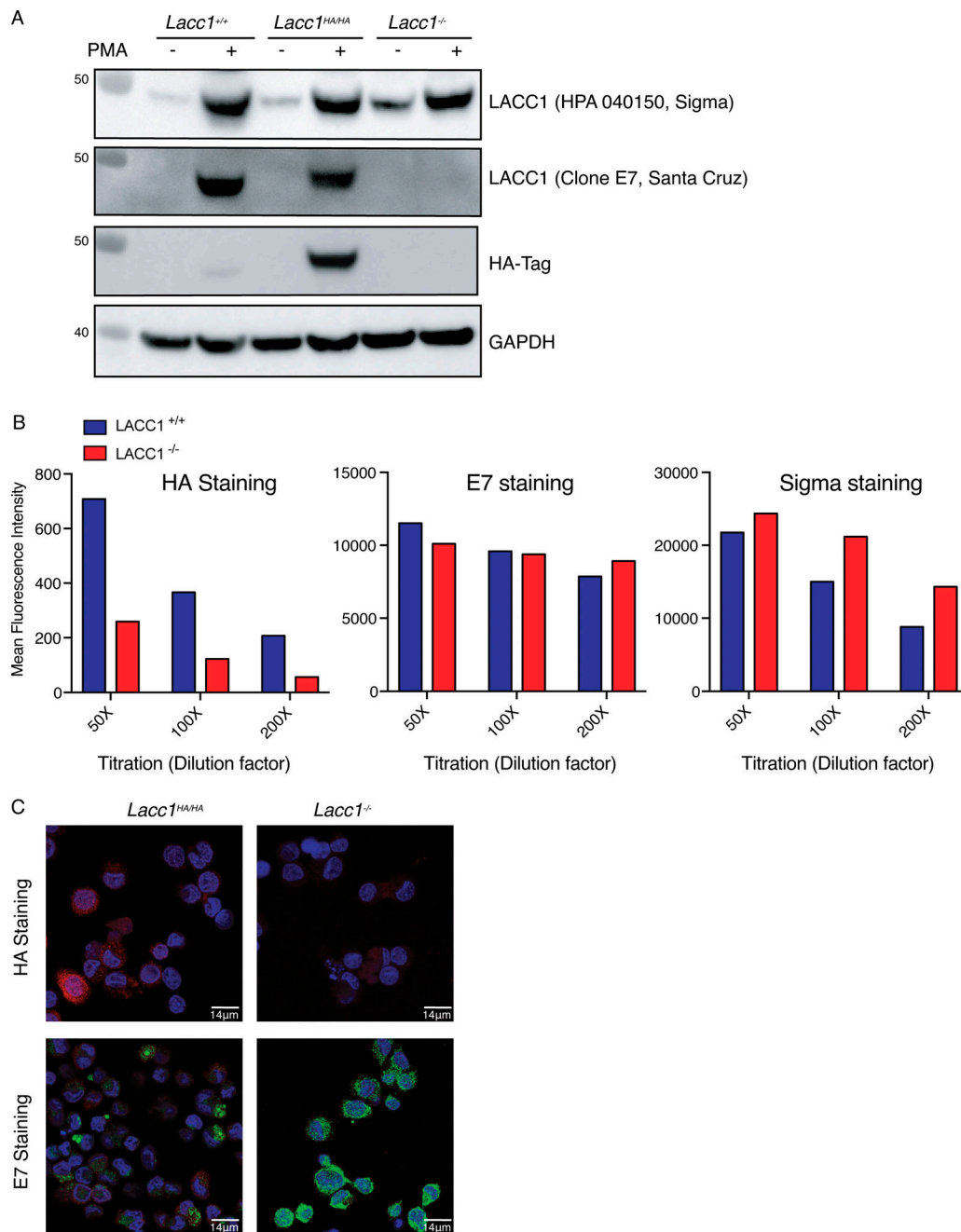


Figure S1. **Endogenous LACC1 tagging reveals unspecific staining by previously used commercial antibodies.** **(A)** Immunoblots of U937 either WT, HA-tagged, or deficient for LACC1 using anti-LACC1 (E7 clone; Santa Cruz), anti-LACC1 (HPA040150; Sigma-Aldrich), or anti-HA (901524; Biolegend) antibody. **(B)** Intracellular FACS staining of U937 HA-LACC1 or LACC1^{-/-} with indicated antibodies against LACC1. **(C)** Confocal analysis of U937 HA-LACC1 or LACC1^{-/-} with indicated antibodies against LACC1. Nucleus was stained with DAPI (blue).

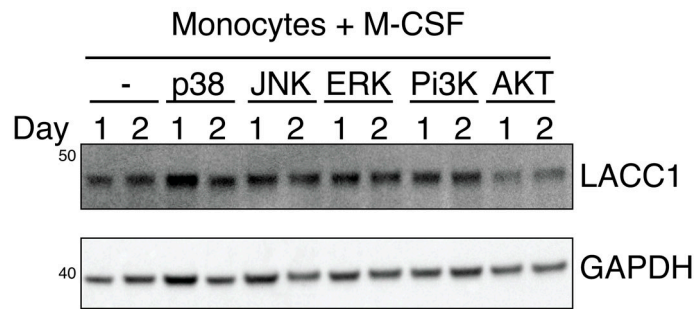


Figure S2. **Role of major signaling pathways on LACC1 expression in macrophages.** Immunoblots of monocytes treated with or without M-CSF and different inhibitors of p38, JNK, ERK, PI3K, and AKT during the indicated period (representative of two experiments).

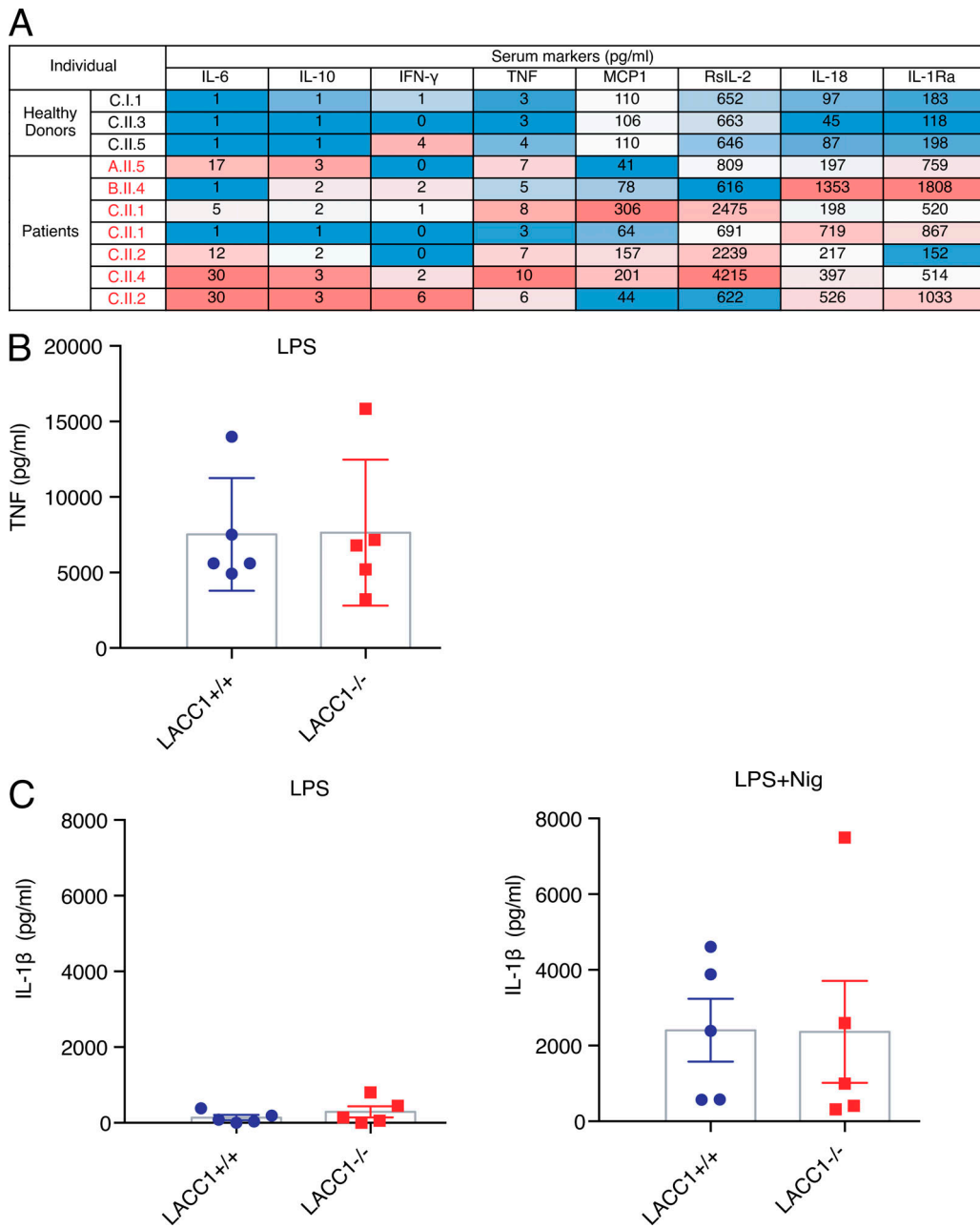


Figure S3. **Inflammatory cytokine production in a LACC1-deficient environment. (A)** Heatmap representation of serum cytokine levels of three healthy family members (black) and seven LACC1 patients (red). **(B)** U937 were differentiated for 48 h with PMA and stimulated 3 h with LPS ($n = 5$). Supernatants were assayed for TNF levels. **(C)** U937 were differentiated for 48 h with PMA and stimulated 3 h with LPS \pm Nigericin (Nig; $n = 5$). Supernatant were assayed for IL-1 β levels.

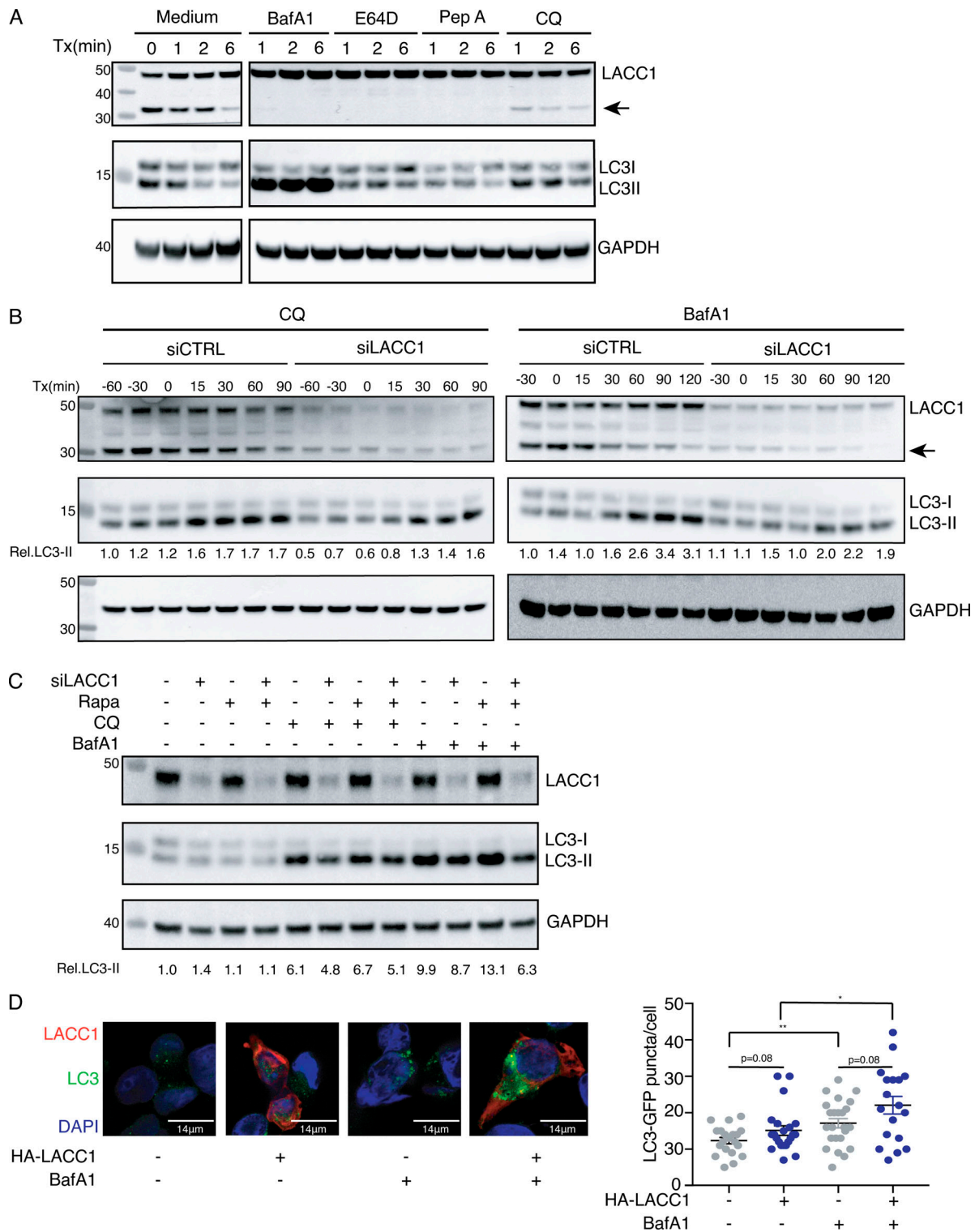


Figure S4. **Autophagy-lysosome inhibitors control LACC1 cleavage and confirms LC3-II accumulation defect in the absence of LACC1.** (A) Immunoblots of M-CSF macrophages treated with or without lysosome-autophagy inhibitors such as Bafilomycin A1 (BafA1), cathepsin inhibitors E64D and pepstatin A (Pep A) or chloroquine (CQ) at different time points (Tx). (B) Immunoblots of siLACC1 macrophages treated with either chloroquine ($n = 2$) or BafA1 ($n = 3$). (C) Immunoblots of siLACC1 macrophages treated with a combination of rapamycin (Rapa), chloroquine, or BafA1 for 2 h ($n = 2$). (D) Confocal microscopy of HeLa cells stably expressing GFP-LC3 (green) transfected with Flag-LACC1 (red). Nucleus was stained with DAPI (blue; representative of three experiments). Right: Quantification of the number of LC3-GFP dots per cell in the different conditions. *, $P < 0.05$; **, $P < 0.005$.

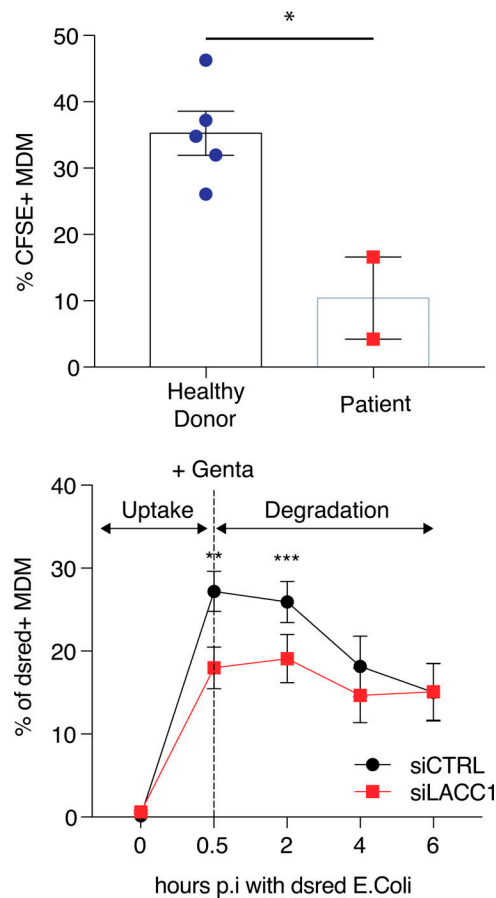


Figure S5. **LACC1-deficient macrophages have impaired capacity to clear apoptotic bodies and bacteria.** **(A)** FACS analysis of five control or two LACC1 patients' macrophages preincubated for 4 h with CFSE-stained apoptotic bodies. **(B)** Control or siLACC1 macrophages were preincubated for 30 min with live DsRed *E. coli* before removal and addition of sterile medium containing antibiotic. Macrophages were analyzed at different time points post infection (p.i.) for bacterial uptake ($n = 4$; *, $P < 0.05$; paired t test). MDM, monocyte-derived macrophage.